

Nonlinear Subdivision Schemes and Multi-Scale Transforms

Nira Dyn and Peter Oswald

1 Introduction

Over the past 25 years, fast multi-scale algorithms such as wavelet-type pyramid transforms for hierarchical data representation, multi-grid solvers for the numerical solution of operator equations, and subdivision methods in computer-aided geometric design lead to tremendous successes in data and geometry processing, and in scientific computing in general. While linear multi-scale analysis is in a mature state [10, 18, 26, 15, 12, 23], not so much is known in the nonlinear case. Nonlinearity arises naturally, e.g. in data-adaptive algorithms, in image and geometry processing, robust de-noising, or due to nonlinear constraints on the analyzed objects themselves that need to be preserved on all scales.

For illustration, and to guide our further discussions, let us introduce three univariate examples of nonlinear multi-scale transforms that have played a central role in the development of the emerging theory.

Example 1: (W)ENO multi-scale transforms for piecewise smooth functions.

Adaption of data representations to jump discontinuities is motivated by applications to hyperbolic PDEs, and serves as simplified model for developing edge-adaptive algorithms in image analysis. Motivated by his work on essentially non-oscillatory (ENO) schemes for numerically solving hyperbolic conservation laws, A. Harten [37, 38, 6] introduced ENO schemes for adaptive multi-scale data representation. For simplicity, assume that a piecewise smooth function $f \in L_\infty(\mathbb{R})$ is sampled at dyadic points, and represented by data vectors $v^j \in \ell_\infty(\mathbb{Z})$ with entries $v_i^j = f(i2^{-j})$ corresponding to uniform grids Γ^j of sampling step-size 2^{-j} . For smooth f , a very popular way to encode the whole sequence $\{v^j\}_{j \geq 0}$ is the

Nira Dyn

Tel Aviv University, School of Mathematical Sciences, e-mail: niradyn@math.tau.ac.il

Peter Oswald

Jacobs University Bremen, School of Engineering and Science, D-28759 Bremen, Germany, e-mail: p.oswald@jacobs-university.de

use of the cubic Deslauriers-Dubuc wavelet transform (sometimes called the standard linear interpolating 4-point scheme, see [20, 21]), where v^j is split into v^{j-1} and the j -th detail sequence d^j given by $d^j = v^j - Sv^{j-1}$, where the linear operator $S: \ell_\infty(\mathbb{Z}) \rightarrow \ell_\infty(\mathbb{Z})$ (called prediction or *subdivision operator*) is given by

$$\begin{aligned} (Sv)_{2i} &= v_i, \\ (Sv)_{2i+1} &= -\frac{1}{16}v_{i-1} + \frac{9}{16}v_i + \frac{9}{16}v_{i+1} - \frac{1}{16}v_{i+2}, \end{aligned} \quad i \in \mathbb{Z}. \quad (1)$$

Indeed, knowing $\{v^0, d^j\}_{j \geq 1}$ allows us to recursively reconstruct the original sequence $\{v^j\}_{j \geq 0}$. Obviously, $d^j_{2i} = 0$ implies that only odd-indexed entries of d^j need to be stored, and storing v^{j-1} and d^j as floating-point numbers is as expensive as storing v^j . Thus, the transform and its finite realizations

$$\{v^j\}_{j=0}^J \longleftrightarrow \{v^0, d^j\}_{j=1}^J, \quad J \geq 1,$$

belong to the class of non-expansive $1-1$ *multi-scale transforms*.

The above S has some properties that are characteristic for most of the multi-scale transforms and are key to their analysis: S is *local* (i.e., data associated with a grid point of Γ^j are predicted from data associated with finitely many grid points of Γ^{j-1} close to it), and *r-shift invariant* with dilation factor $r = 2$. The latter property can be formalized by the operator identity $ST_k = T_kS$, where T_k is the shift-operator given by $(T_kv)_i = v_{i+k}$, $i \in \mathbb{Z}$. Another property that is central to the subject is the *polynomial reproduction* and, closely related, *approximation order* of S . Detailed definitions will be given later. For the above S it is well-known that it reproduces cubic polynomials because the formula for $(Sv^{j-1})_{2i+1}$ comes from interpolating the four data $\{v_s^{j-1}\}_{s=i-1, \dots, i+2}$ at the corresponding sub-grid of Γ^{j-1} by a cubic polynomial p_i , and evaluating its value at the point $(i + \frac{1}{2})2^{-j+1}$ of Γ^j central to them. As a result, for smooth f the ℓ_p norms of the detail sequences d^j decay at a rate 2^{-4j} . Thus, if representation is required up to a certain accuracy only then fewer bits are necessary to encode the detail information.

This savings effect is to some extent lost when jump discontinuities are present. A remedy is to detect potential jump discontinuities from the data v^{j-1} , and use a smarter, data-dependent and thus nonlinear, prediction rule. For ENO schemes, one chooses the "least oscillating" among the interpolating cubic polynomials p_{i-1} , p_i , p_{i+1} for assigning an appropriate value corresponding to the point $(i + \frac{1}{2})2^{-j+1}$. The effect of this modification is illustrated in Fig. 1, the nonlinear scheme obviously suppresses the spurious oscillations associated with the Gibbs phenomenon for linear wavelet-type transforms, and reduces the number of large detail entries d_i^j near the jump discontinuity.

Weighted essentially non-oscillatory (WENO) transforms use a convex combination of the three predictions, with weights smoothly depending on the measured oscillations. Instead of interpreting the entries v_i^j as values of f at dyadic points $i2^{-j}$, one could equally well interpret them as average on dyadic intervals $(i2^{-j}, (i+1)2^{-j})$. In this case other subdivision operators S would be preferable for symmetry reasons, and the restriction would be more naturally defined by averaging

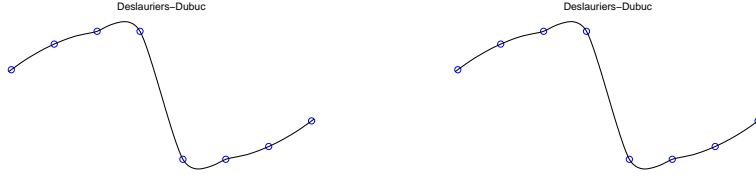


Fig. 1 While the linear Deslauriers-Dubuc subdivision scheme produces overshoots near a jump (left), the nonlinear ENO scheme avoids artifacts (right) but produces a less smooth limit near the jump. The coarse grid data points are indicated by circles.

$v_i^{j-1} = (v_{2i}^j + v_{2i+1}^j)/2$ rather than by simple down-sampling. The convergence, limit smoothness, and stability properties of these schemes have been systematically studied in [13] within a framework of *quasi-linear, data-dependent subdivision* which will be reviewed in below. Functional limits of the sequence $\{v^j\}_{j \geq 0}$ are understood in the usual way as limits of an associated sequence $\{f^j\}_{j \geq 0}$, where the function $f^j \in C(\mathbf{R})$ is typically defined as the linear spline interpolant to the data (Γ^j, v^j) . We note that there exist other families of nonlinear schemes of a similar flavor (e.g., monotonicity and convexity preserving schemes, PPH, and power- p schemes, see e.g. [43, 46, 5, 2]).

Example 2: Median-interpolating schemes for robust de-noising. In [22], motivated by applications to heavy-tail, non-Gaussian noise removal, a nonlinear multi-scale transform with dilation factor $r = 3$ was introduced where point evaluations and linear averaging operations are systematically replaced by median calculations. More precisely, let us assume that the entries v_i^j of the fine-scale data vector v^j represent noisy measurements of average values on triadic intervals $I_i^j = (i3^{-j}, (i+1)3^{-j})$ of a smooth function f . Then, [22] uses the rule

$$v_i^{j-1} = \text{med}(v_{3i}^j, v_{3i+1}^j, v_{3i+2}^j), \quad i \in \mathbb{Z}, \quad j = 1, \dots, J, \quad (2)$$

to define coarse-scale representations of the measured data (the median of three numerical values is defined in the obvious way). Detail sequences d^j are formally defined by $d^j = v^j - Sv^{j-1}$, $j = 1, \dots, J$, as before but using a new type of nonlinear *median-interpolating subdivision operator* S . To define it, recall that the values $\{v_s^{j-1}\}_{s=i-1, i, i+1}$ can be interpreted as approximate coarse-scale medians of f on the three consecutive intervals I_s^{j-1} , $s = i-1, i, i+1$. It turns out that there is a unique quadratic polynomial p_i whose median with respect to these three intervals coincides with the given v_s^{j-1} , $s = i-1, i, i+1$, i.e.,

$$p_i(t) = At^2 + Bt + C : \quad v_s^{j-1} = \text{med}(p_i; I_s^{j-1}), \quad s = i-1, i, i+1. \quad (3)$$

Then, for the three subintervals of I_i^{j-1} with respect to the next triadic grid, set

$$(Sv^{j-1})_s := \text{med}(p_i; I_s^j), \quad s = 3i, 3i+1, 3i+2. \quad (4)$$

Note that this subdivision scheme is closely related to a linear scheme which one obtains if one replaces the median conditions in both the interpolation step (3) and the imputation step (4) by evaluation at the corresponding interval midpoints (for a monotone continuous function f on an interval I , the median indeed coincides with the value of f at the midpoint of I). The idea of studying nonlinear subdivision processes and multi-scale transforms by relating them to close-by linear schemes, and using perturbation arguments is very fruitful, and has been followed by various authors [25, 65, 62, 61, 19].



Fig. 2 The rules for the nonlinear median-interpolating subdivision scheme (left), and the linear midpoint-interpolating scheme (right) are close but not identical.

The convergence and smoothness properties of the limits of the median-interpolating subdivision process have been studied in a series of papers [22, 52, 64], for the stability of the associated multi-scale transform, see [36]. The remarkable paper [64] solves the smoothness problem in the Hölder scale, and is based on a detailed analysis of associated nonlinear dynamical systems. Various extensions of the median-interpolating multi-scale transform have been proposed as well: one can consider higher-order median-interpolation [30], other robust estimators [53] or nonlinear interpolation conditions [51, 65].

Example 2 is an *expansive multi-scale transform*. Indeed, an easy calculation shows that the 3^J data per unit interval to be stored for v^J are replaced by $1 + 3 + \dots + 3^J \approx 3^{J+1}/2$ data to be stored for $\{v^0, d^j\}_{j=1}^J$ resulting in an increase of storage requirements by a factor $3/2$. Expansive multi-scale transforms occur also if linear frame representations are explored, and offer sometimes even some advantages (e.g., robustness with respect to erasures in the case of frame decompositions).

Example 3: Normal multi-resolution for efficient geometry compression. While the previous examples serve scalar data associated with the (appropriately interpreted) samples of a function with respect to a uniform grid (a situation which we call *functional setting*), in geometry processing there is no fixed or natural parametrization of a geometric object by a function, and finding an appropriate parametrization is often part of the processing task. Normal multi-resolution is a remarkable example of a nonlinear multi-scale transform that has originally been developed for surface compression [41, 34] and image analysis [39], works directly on vector data, and cannot be reduced to the scalar case. It serves as an example for what we call *geometric nonlinear multi-scale transforms*. To reveal the main idea, we describe the scheme for representing a closed smooth curve \mathcal{C} embedded

into \mathbf{R}^2 for $r = 2$ following [19, 55]. The scalar-valued data vectors $v^j \in \ell_\infty(\mathbb{Z})$ from the previous examples will be replaced by \mathbf{R}^2 -valued periodic sequences \mathbf{v}^j of length $2^j n_0$ with $n_0 \geq 3$, which consist of points \mathbf{v}_i^j on \mathcal{C} . Periodicity means that $\mathbf{v}_{i+2^j n_0}^j \equiv \mathbf{v}_i^j$ for all $i \in \mathbb{Z}$. The analysis step of the normal multi-resolution scheme starts with a sufficiently dense sampling \mathbf{v}^0 of $n_0 \geq 3$ curve points ordered such that the polygonal line obtained by connecting consecutive \mathbf{v}_i^0 by straight line segments is a faithful approximation to \mathcal{C} . To construct \mathbf{v}^j from \mathbf{v}^{j-1} , we keep the curve points from \mathbf{v}^{j-1} by setting $\mathbf{v}_{2i}^j = \mathbf{v}_i^{j-1}$ for all $i \in \mathbb{Z}$, and insert new points $\mathbf{v}_{2i+1}^j \in \mathcal{C}$ by first predicting "base points" $\hat{\mathbf{v}}_{2i+1}^j$ using any reasonable interpolating subdivision operator S , i.e., $\hat{\mathbf{v}}^j = S\mathbf{v}^{j-1}$. The point \mathbf{v}_{2i+1}^j is obtained by intersecting the normal to the edge vector $\mathbf{e}_i^{j-1} := \mathbf{v}_{i+1}^{j-1} - \mathbf{v}_i^{j-1}$ through the base point $\hat{\mathbf{v}}_{2i+1}^j$ with \mathcal{C} . We do not dwell on implementation aspects such as the subtle issue of which curve point to select if there are many intersection points. What needs to be stored as entry d_i^j of the detail sequence d^j is the signed distance of \mathbf{v}_{2i+1}^j from the base point $\hat{\mathbf{v}}_{2i+1}^j$. The reconstruction (or synthesis) step $\{\mathbf{v}^0, d^j\}_{j=1}^J \mapsto \mathbf{v}^J$ is recursively given by

$$\mathbf{v}_{2i}^j = \mathbf{v}_i^{j-1}, \quad \mathbf{v}_{2i+1}^j = (S\mathbf{v}^{j-1})_{2i+1} + d_i^j \mathbf{n}_i^{j-1}, \quad i = 0, \dots, 2^{j-1} n_0,$$

for $j = 1, \dots, J$, where

$$\mathbf{n}_i^{j-1} := \|\mathbf{e}_i^{j-1}\|^{-1} (\mathbf{e}_i^{j-1})^\perp$$

denotes the unit normal vector to the edge vector \mathbf{e}_i^{j-1} . This time, the nonlinearity is hidden in the normal computation for the detail update, and not in the subdivision part as in the previous examples. Fig. 3 illustrates the construction.

Normal multi-resolution offers two obvious advantages. First of all, for smooth \mathcal{C} and appropriate S , choosing the locally geometry-adapted frame consisting of the edge/normal vector pairs $(\mathbf{e}_i^{j-1}, \mathbf{n}_i^{j-1})$ results in much smaller detail magnitudes than using fixed coordinate axes for all $i \in \mathbb{Z}$, and, more importantly, the detail sequences contain scalar data. Indeed, the representation of the curve by its fine-scale sampling \mathbf{v}^J requires $2^{J+1} n_0$ reals while its multi-scale $\{\mathbf{v}^0, d^j\}_{j=1}^J$ is given by $2n_0 + (1 + \dots + 2^{J-1})n_0 \approx 2^J n_0$ reals. The savings are even more impressive when the idea is applied to surfaces and piecewise smooth multivariate functions, and combined with compression by thresholding detail entries d_i^j , see the performance reports in [41, 34, 39]. The papers [19, 55] give the analysis of normal multi-scale transforms with a linear interpolating subdivision operator S for the case of smooth curves based on perturbation arguments. The surface case still awaits its theoretical analysis.

In general, nonlinear multi-scale transforms operate on grid functions $\Gamma^j \rightarrow X$, where X typically coincides with \mathbf{R}^n for some $n \geq 1$ (or with a manifold embedded into \mathbf{R}^n). The grids Γ^j are generated in a systematic way by a certain *topology refinement* (data-adapted topology refinement is an area of future research). In the above examples, $\Gamma^j = r^{-j}\mathbb{Z}$ is created by uniform r -adic refinement for $r = 2$, resp.

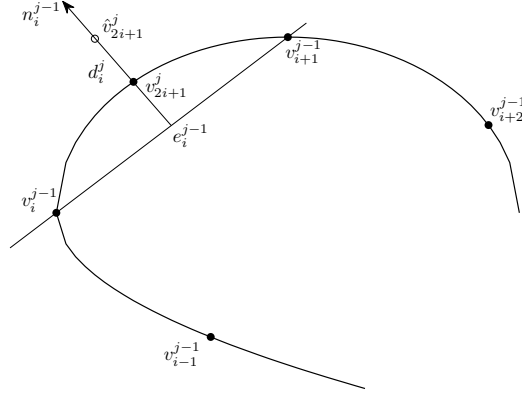


Fig. 3 Illustration of the normal multi-resolution scheme.

$r = 3$. In the multivariate case, much more general grid topologies and refinement rules are possible. The values of the grid functions are collected into vectors v^j with entries indexed by the elements of Γ^j . They are related to each other by down-sampling operations using restriction operators R_j ,

$$v^{j-1} = R_j v^j, \quad j \geq 1, \quad (5)$$

detail computations

$$d^j = D_j(v^j, v^{j-1}, S_j v^{j-1}), \quad j \geq 1, \quad (6)$$

involving prediction or subdivision operators S_j , and up-sampling operations

$$v^j = P_j(v^{j-1}, d^j) \quad j \geq 1, \quad (7)$$

where at least one of these components involves nonlinear maps. In our univariate examples, we can use the fact that all Γ^j are isomorphic to \mathbb{Z} , and interpret the data vectors v^j as elements of $\ell_\infty(\mathbb{Z} \rightarrow X)$, where $X = \mathbb{R}$ in Example 1 and 2, and $X = \mathbb{R}^2$ for Example 3. This allows us to work with operators R , S , D , and P that act on this sequence space, and do not depend on j . For Example 1, the operator R is given by $(Rv)_i = v_{2i}$, is linear, and corresponds to trivial down-sampling for $r = 2$, while S is the ENO-modified nonlinear Deslauriers-Dubuc subdivision operator, $D(\tilde{v}, v, \hat{v}) := \tilde{v} - \hat{v}$, and $P(v, d) = Sv + d$. For Example 3, $X = \mathbb{R}^2$, R is as above, S is the linear Deslauriers-Dubuc subdivision operator, while the nonlinearity is induced through the normal map $v \rightarrow \mathbf{n}(v)$ that enters the detail computation,

and up-sampling operation:

$$D(\tilde{v}, v, \hat{v})_i := (\tilde{v} - \hat{v})_i \cdot \mathbf{n}(v)_i, \quad i \in \mathbb{Z},$$

$$P(v, d)_{2i} = (Sv)_{2i} = v_i, \quad P(v, d)_{2i+1} = (Sv)_{2i+1} + d_i \mathbf{n}_i, \quad i \in \mathbb{Z}.$$

Finally, Example 2 is characterized by nonlinear R given by (2), and nonlinear S given by (3-4), while D and P remain the same as in Example 1.

The theoretical investigation of the properties of a nonlinear transform

$$v^J \longleftrightarrow \{v^0, d^1, \dots, d^J\}, \quad J \geq 1, \quad (8)$$

requires the study of the limit behavior for $J \rightarrow \infty$, and concentrates on answering the following natural questions:

- **Convergence.** Given reasonable v^0 and d^j , $j \geq 1$, do the reconstructed v^j converge to a reasonable limit object? This can be cast in terms of convergence of the associated sequence of functions f^j to a limit f^∞ in some function space.
- **Smoothness.** To judge the visual appearance of the results of reconstruction (for instance after a compression step), or in applications to numerical discretization schemes for elliptic boundary value problems, the guaranteed smoothness of these limits f^∞ in the Hölder or Sobolev scale is of essential interest.
- **Approximation and detail decay.** If the limit object f^∞ is sufficiently smooth, can we guarantee that the functions f^j that represent the grid data v^j converge to f^∞ at a certain prescribed rate typical for this smoothness class and comparable linear approximation processes? A related question is whether the smoothness properties of f^∞ can be characterized in terms of the detail sequences d^j , $j \geq 1$, as is well-known for many linear wavelet transforms.
- **Stability.** While the stability of the decomposition step

$$v^J \longrightarrow \{v^0, d^1, \dots, d^J\}, \quad J \geq 1,$$

(small perturbations in the fine-grid data v^J for J large will not lead to big perturbations of the details d^j , $j \leq J$, or the coarse grid data v^0) is often easy to understand (e.g., for interpolatory transforms when trivial down-sampling is used), the stability of the multi-scale reconstruction step

$$\{v^0, d^1, \dots, d^J\} \longrightarrow v^J, \quad J \geq 1,$$

is a difficult question of extreme importance for introducing compression strategies based on thresholding of detail sequences in a multi-scale decomposition.

Our aim is to survey the existing case studies for nonlinear multi-scale transforms and the emerging approaches to the development of a theory that tries to give first answers to the above questions. The exposition concentrates on the univariate case, namely multi-scale processing of data sampled from univariate functions or from curves. It is split into presenting the basic theory of nonlinear transforms in the functional setting in section 2 (this covers Example 1 and 2), and an exemplary

discussion of what we call geometric subdivision schemes and multi-scale transforms, for which Example 3 is prototypical, in section 3. Extensions to multivariate schemes, schemes that process manifold- or set-valued data, and some other recent developments will not be reviewed. This way, we hope to be able to expose the main ideas more clearly, and still provide enough guidance for future research in this exciting research field.

2 Nonlinear Multi-Scale Transforms: Functional Setting

2.1 Basic Notation and Further Examples

Throughout Section 2, we consider local, r -shift invariant, stationary multi-scale transforms (8), recursively acting on data sequences from $\ell_p(\mathbb{Z})$ ($1 \leq p \leq \infty$) according to a simplified version of (5), (6), (7), where

$$v^{j-1} = Rv^j, \quad d^j = D(v^j - Sv^{j-1}); \quad v^j = Sv^{j-1} + Pd^j, \quad j \geq 1, \quad (9)$$

with bounded but generally nonlinear operators $P, D, R, S : \ell_p(\mathbb{Z}) \rightarrow \ell_p(\mathbb{Z})$. Abusing a bit conventions in the nonlinear case, we call an operator $T : X \rightarrow Y$ between two Banach space X and Y bounded if there is a constant C_0 such that $\|Tx\|_Y \leq C_0\|x\|_X$ for all $x \in X$, and Lipschitz continuity of such a T always means that there exists a constant C_1 such that $\|Tx - Tx'\|_Y \leq C_1\|x - x'\|_X$ for all $x, x' \in X$. For consistency in (9), the relation $(\text{Id} - PD)(\text{Id} - SR) = 0$ needs to hold. Here Id is the identity operator. That the operators in (9) are independent of the scale index $j \geq 1$ makes the scheme stationary. Example 1 and 2 from Section 1 fit this definition (for them $P = D = \text{Id}$).

Example 4. Second generation linear and nonlinear wavelet transforms. Here is the construction of a 2-shift invariant univariate 1 – 1 multi-scale transform from [8] based on the lifting scheme [59, 60]. Let v^j be split into "even" and "odd" parts

$$(R_e v^j)_i := v_{2i}^j, \quad (R_o v^j)_i := v_{2i+1}^j, \quad i \in \mathbb{Z}.$$

Then set

$$d^j := R_o v^j - T_{c,1} R_e v^j, \quad v^{j-1} := R_e v^j + T_{c,2} d^j \quad (10)$$

for decomposition and

$$R_e v^j = v^{j-1} - T_{c,2} d^j, \quad R_o v^j := d^j + T_{c,1} R_e v^j \quad (11)$$

for reconstruction. Here,

$$(T_{c,s} v)_i = \sum_{k=-K_1}^{K_2} b_{s;k}(v_{i-K_1}, \dots, v_{i+K_2}) v_{i-k}, \quad i \in \mathbb{Z},$$

are linear or nonlinear convolution operators generated by finitely many coefficient functions $b_{s,k} : \mathbb{R}^{K_1+K_2+1} \rightarrow \mathbb{R}$, $k = -K_1, \dots, K_2$, $s = 1, 2$. This is called "predict first" transform in [8], another "update first" transform is obtained by switching the order of execution of the sub-steps in (10), (11):

$$v^{j-1} := R_e v^j + T_{c,2} R_o v^j, \quad d^j := R_o v^j - T_{c,1} v^{j-1}, \quad (12)$$

$$R_o v^j := d^j + T_{c,1} v^{j-1}, \quad R_e v^j = v^{j-1} - T_{c,2} d^j, \quad (13)$$

Concrete examples, e.g., multi-scale transforms, where the nonlinearity is induced by quantization, or ENO-type schemes working with variable-order interpolating polynomials near a suspected jump discontinuity, and references can be found in [8].

Both transforms can be rewritten in our standard form (9), e.g., for the "predict first" version, one would set $R = (\text{Id} - T_{c,2} T_{c,1}) R_e + T_{c,2} R_o$, $D = -T_{c,1} R_e + R_o$, and define S and P by

$$R_e S = \text{Id}, \quad R_o S = T_{c,1}, \quad R_e P = -T_{c,2}, \quad R_o P = \text{Id} - T_{c,1} T_{c,2}.$$

General linear bi-orthogonal wavelet transforms [18, 15] with finitely supported masks have similar representations, with all involved operators being linear. Transforms of the above type are obviously non-expansive $1 - 1$ transforms, i.e., do not formally change storage requirements. Note that there is also growing interest in expansive transforms related to tight affine frames. Lack of space prevents us from giving further details.

Example 5. Power- p schemes. This multi-scale transform is similar to Example 1 but uses a different prediction rule. I.e., again $r = 2$, $P = D = I$, the restriction operator is given by $(Rv)_i = v_{2i}$, $i \in \mathbb{Z}$, and the interpolating subdivision operator S is given by

$$(Sv)_{2i} = v_i, \quad (Sv)_{2i+1} = \frac{v_i + v_{i+1}}{2} - \frac{1}{8} H_p(\Delta^2 v_{i-1}, \Delta^2 v_i), \quad i \in \mathbb{Z}, \quad (14)$$

where the so-called limiter H_p is defined by

$$H_p(x, y) = \begin{cases} \frac{x+y}{2} \left(1 - \left| \frac{x-y}{x+y} \right|^p \right), & xy > 0, \\ 0, & xy \leq 0. \end{cases} \quad (15)$$

The parameter $p \in [1, +\infty)$ is fixed, $\Delta^k := (\Delta)^k$ denotes the k -th order forward difference operator acting on sequence spaces, where $(\Delta v)_i = v_{i+1} - v_i$, $i \in \mathbb{Z}$.

Power- p schemes have been introduced in the context of generalized ENO-methods for hyperbolic problems [58], and can be useful for compressing piecewise smooth data and functions. Earlier, the case $p = 2$ appeared in [29, 43]. A straightforward calculation shows that if $v|_{\{i_0, \dots, i_1\}}$ is a convex (concave, linear) segment

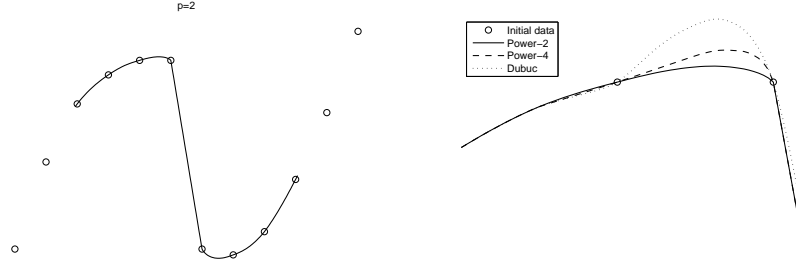


Fig. 4 Limits of power-2 subdivision (on the left), and a comparison with power-4 subdivision and the cubic Deslauriers-Dubuc scheme near a jump (on the right)

of v , then $(Sv)|_{\{2i_0, \dots, 2i_1\}}$ preserves this property if $p \in [1, 2]$. The formula is constructed such that for $\Delta^2 v_{i-1} = \Delta^2 v_i$ the obtained value $(Sv)_{2i+1}$ is the same as for the linear interpolating cubic Deslauriers-Dubuc 4-point scheme discussed in Example 1 while at intervals, where the sign of the second differences changes, the newly inserted value is obtained by linear interpolation from its endpoint values.

Coming back to the notation for the r -shift invariant univariate case, the grids $\Gamma^j = r^{-j}\mathbb{Z}$ are systematically identified with \mathbb{Z} , the subdivision operator $S : \ell_p(\mathbb{Z}) \rightarrow \ell_p(\mathbb{Z})$ satisfies $ST_k = T_{rk}S$, and the restriction operator $R : \ell_p(\mathbb{Z}) \rightarrow \ell_p(\mathbb{Z})$ satisfies $RT_{kr} = T_kR$. The locality of an r -shift invariant transform is assured by assuming that the action of S is given by r multivariate functions ϕ_s according to

$$(Sv)_{ri+s} = \phi_s(v_{i-L_1}, \dots, v_{i+L_2}), \quad s = 0, \dots, r-1, \quad (16)$$

where the integers L_1, L_2 are fixed and independent of $i \in \mathbb{Z}$, and $L = L_1 + L_2 + 1$ is the support length of the subdivision part of the transform. Similarly,

$$(Rv)_i = \phi(v_{ri-L_3}, \dots, v_{ri+L_4}) \quad (17)$$

for some function ϕ and fixed integers L_3, L_4 . It is easy to see that due to locality and r -shift invariance, boundedness (Lipschitz continuity, C^1 property, ...) of S on $\ell_p(\mathbb{Z})$ spaces is equivalent to the boundedness (Lipschitz continuity, C^1 property, ...) of the coordinate functions $\phi_s : \mathbb{R}^L \rightarrow \mathbb{R}$ representing S , similarly for R . We will always silently assume that $S\mathbf{0} = R\mathbf{0} = \mathbf{0}$, where $\mathbf{0}$ is the zero sequence given by $\mathbf{0}_i = 0, i \in \mathbb{Z}$.

Sometimes, especially if nonlinear schemes are considered as perturbations of associated linear schemes, the alternative representation

$$(Sv)_{ri+s} = \sum_{l=-L_2}^{L_1} a_{rl+s}(v_{i-L_1}, \dots, v_{i+L_2})v_{i-l}, \quad s = 0, \dots, r-1,$$

or, equivalently,

$$(Sv)_j = \sum_{i \in \mathbb{Z}} a_{j-ri} (v|_{I_{[j/r]}}) v_i, \quad j \in \mathbb{Z}, \quad (18)$$

is chosen. To shorten the notation, by $v|_{I_i}$ we have denoted the restriction of v to the finite index set $I_i := \{i - L_1, \dots, i + L_2\}$, $i \in \mathbb{Z}$. Coefficient functions with index $s \notin \{-rL_1, \dots, r(L_2 + 1) - 1\}$ vanish for all arguments: $a_s(\cdot) \equiv 0$. Based on (18) we can now formally write the action of S as an infinite matrix-vector product

$$Sv = S_v v, \quad (19)$$

where S_v is a bi-infinite, data-dependent matrix operator with entries identified from (18):

$$(S_v)_{j,i} := a_{j-ri} (v|_{I_{[j/r]}}), \quad j, i \in \mathbb{Z}.$$

Note that for a linear S , the matrix operator S_v do not depend on v (in which case we can drop the subscript v , and identify S with its matrix representation), and is given by the finitely supported sequence $a := \{a_l\}_{l \in \mathbb{Z}}$ called *mask* of the subdivision operator. The representation (18)-(19) was introduced in [13], and was the departure point for a systematic theory of data-dependent, so-called quasi-linear, subdivision schemes and multi-scale transforms which will be reviewed below. The transition from (16) to (18) and (19) is not unique, and needs to be done carefully.

Another often used approach is to write $S = S_0 + T'$, where S_0 is an appropriate linear subdivision operator and the remaining nonlinear part T' is "small" in a certain sense, see [19, 51, 2] for this perturbation approach. E.g., the power- p subdivision scheme from Example 5 naturally splits into a linear part S_0 (point insertion by linear interpolation) and nonlinear perturbation T' given by the limiter, and depending only on the 2nd order differences $\Delta^2 v$. For the median-interpolating scheme of Example 2, the natural choice for S_0 is the linear midpoint interpolation scheme given by

$$(S_0 v)_{3i+s} = \begin{cases} \frac{2v_{i-1} + 8v_i - v_{i+1}}{9}, & s = 0, \\ v_i, & s = 1, \\ \frac{-v_{i-1} + 8v_i + 2v_{i+1}}{9}, & s = 2, \end{cases} \quad i \in \mathbb{Z},$$

and the resulting perturbation operator $T' = S - S_0$ given by

$$(T' v)_{3i+s} = \alpha_s (\Delta v|_{\{i-1, i\}}) \Delta^2 v_i, \quad s = 0, 1, 2, \quad i \in \mathbb{Z},$$

depends in a specific way on Δv and $\Delta^2 v$ (e.g., the functions α_s are uniformly bounded, see [52, Section 2.2] for details). To identify the representation (16) from these formulas, set $L_1 = L_2 = 1$.

For the latter scheme, a natural choice for the representation (18), (19) is to set

$$a_{3l} = \begin{cases} \frac{2}{9} + \alpha_0(\cdot), \\ \frac{8}{9} - 2\alpha_0(\cdot), \\ -\frac{1}{9} + \alpha_0(\cdot), \end{cases} \quad a_{3l+1} = \begin{cases} \alpha_1(\cdot), \\ 1 - 2\alpha_1(\cdot), \\ \alpha_1(\cdot), \end{cases} \quad a_{3l+2} = \begin{cases} -\frac{1}{9} + \alpha_2(\cdot), & l = 1, \\ \frac{8}{9} - 2\alpha_2(\cdot), & l = 0, \\ \frac{2}{9} + \alpha_2(\cdot), & l = -1. \end{cases}$$

The non-zero entries of the matrix representation of S_v are contained in the 3×3 sub-blocks

$$(S_v)|_{\{3i, 3i+1, 3i+2\} \times \{i-1, i, i+1\}} = \begin{pmatrix} a_3(\Delta v|_{\{i-1, i\}}) & a_0(\Delta v|_{\{i-1, i\}}) & a_{-3}(\Delta v|_{\{i-1, i\}}) \\ a_4(\Delta v|_{\{i-1, i\}}) & a_1(\Delta v|_{\{i-1, i\}}) & a_{-2}(\Delta v|_{\{i-1, i\}}) \\ a_5(\Delta v|_{\{i-1, i\}}) & a_2(\Delta v|_{\{i-1, i\}}) & a_{-1}(\Delta v|_{\{i-1, i\}}) \end{pmatrix},$$

$i \in \mathbb{Z}$. In the general case, (18) results in a similar block-structured matrix operator S_v with $r \times (L_1 + L_2 + 1)$ sub-blocks.

Explicit representations (18), (19) have also been used in the study of (W)ENO schemes in [13] (for WENO, see also [2, Section 4.2]). Within the framework of Example 1, formulas for $a_s(\cdot)$ and S_v follow from

$$(Sv)_{2i+1} := \sum_{l=-1}^1 c_{-l}(\Delta v|_{\{i-2, \dots, i+2\}})(S_l v)_{2i+l} \quad (20)$$

where S_0 is the standard 4-point scheme (1) while the formulas

$$(S_l v)_{2i+1} = \begin{cases} \frac{v_{i-2} - 5v_{i-1} + 10v_i + 4v_{i+1}}{16}, & l = 1 \\ \frac{-v_{i-2} + 9v_{i-1} + 9v_i - v_{i+1}}{16}, & l = -1 \end{cases} \quad i \in \mathbb{Z}.$$

define the linear schemes obtained from predictions using shifted cubic interpolation polynomials $p_{i\pm 1}$ (all schemes are considered interpolating, i.e., $(Sv)_{2i} = (S_l v)_{2i} = v_i$, $i \in \mathbb{Z}$, $l = -1, 0, 1$). For WENO, the coefficient functions

$$c_l(\cdot) := \frac{\alpha_l(\cdot)}{\alpha_{-1}(\cdot) + \alpha_0(\cdot) + \alpha_1(\cdot)}, \quad \alpha_l(\cdot) := \left(\frac{\beta_l}{\varepsilon + \beta_l(\cdot)} \right)^2,$$

depend on non-negative, smooth functions $\beta_l(\cdot)$ measuring for argument $\Delta v|_{\{i-2, \dots, i+2\}}$ the degree of oscillation of the prediction polynomial p_{i+l} , and $\varepsilon, \beta_l > 0$ are fixed constants, $l = -1, 0, 1$. The small parameter $\varepsilon > 0$ acts as regularization parameter, and avoids division by zero. Obviously, $c_l(\cdot) \in (0, 1)$ and $c_1(\cdot) + c_0(\cdot) + c_{-1}(\cdot) = 1$, i.e., the WENO subdivision operator (20) is a convex combination of the three linear operators S_l , with coefficients smoothly depending on Δv . The ENO subdivision operator has the same principal structure (20) but a generally discontinuous dependence of the coefficients $c_l(\cdot)$ on $\Delta(v)$: For ENO, we set $c_l(\Delta v|_{\{i-2, \dots, i+2\}}) = 1$ if p_{i+l} is the least oscillating of the three predictor polynomials, i.e., if $\beta_l(\Delta v|_{\{i-2, \dots, i+2\}})$ is minimal, and assign zeros to the other two coefficients. For these so-called 6-point (W)ENO schemes, set $L_1 = 2$, $L_2 = 3$ in (18).

This following subsections represent a summary of the currently available theoretical results for the family (9) of nonlinear multi-scale transforms and associated subdivision processes $v^j = Sv^{j-1}$, $j \geq 1$, which is obtained from (9) by formally setting $d^j = \mathbf{0}$ for $j \geq 1$. We survey mainly results from [13, 49, 19, 64, 52, 36, 2], where proofs and further material can be found. A few results, especially on offset

invariant S , and extensions to $L_p(\mathbf{R})$ for $1 \leq p < \infty$, are new and elaborated on in more detail in a forthcoming paper.

2.2 Polynomial Reproduction and Derived Subdivision Schemes

The concept of polynomial reproduction for subdivision operators is fundamental in the study of multi-scale transforms, therefore we start the exposition with it. For nonlinear S , there are two slightly different extensions of the familiar definition for linear subdivision operators. The first definition follows [13], the second [64, 36]. Throughout the section, we denote by \mathbf{P}_k the set of algebraic polynomials of degree $< k$ or, equivalently, of order $\leq k$, and by $\mathbf{1}$ the constant sequence given by $\mathbf{1}_i := 1$, $i \in \mathbb{Z}$.

Definition 1. Let the r -shift invariant subdivision operator S be represented in the form (19). Then S has polynomial reproduction of order $k \geq 1$ if for each $v \in \ell_p(\mathbb{Z})$ the associated linear subdivision operator S_v has the following property: For any polynomial p of degree m , $0 \leq m < k$, there exists a polynomial q of degree $< m$ such that

$$S_v(p|\mathbf{z}) = (p+q)|_{r^{-1}\mathbf{z}}.$$

In particular, S reproduces constants (i.e., has polynomial reproduction of order $k = 1$) if

$$S_v(\mathbf{1}) = \mathbf{1}, \quad \forall v \in \ell_p(\mathbb{Z}).$$

Definition 2. An r -shift invariant subdivision operator S is offset invariant for \mathbf{P}_k , $k \geq 1$, if for each $v \in \ell_p(\mathbb{Z})$, and any polynomial p of degree m , $0 \leq m < k$, there exists a polynomial q of degree $< m$ such that

$$S(v+p|\mathbf{z}) = Sv + (p+q)|_{r^{-1}\mathbf{z}}.$$

In particular, S is offset invariant for constants (i.e., the set \mathbf{P}_1) if

$$S(v + \alpha\mathbf{1}) = Sv + \alpha\mathbf{1}, \quad \forall \alpha \in \mathbf{R}, \quad \forall v \in \ell_p(\mathbb{Z}).$$

Note that the formulation of these definitions automatically ensures that polynomial reproduction of order k implies polynomial reproduction of order m (similarly offset invariance for \mathbf{P}_k implies offset invariance for \mathbf{P}_m) for all $1 \leq m < k$. For linear S , both definitions coincide. As Example 1 and 2 demonstrate, for nonlinear schemes the two conditions are different. E.g., since the (W)ENO subdivision operator (20) is a convex combination of three linear subdivision operators, each being exact for cubic polynomials, it possesses polynomial reproduction of order $k = 4$. On the other hand, although it is obviously offset invariant for \mathbf{P}_1 (because the coefficient functions depend on Δv , and not on v directly), it is not offset invariant for any \mathbf{P}_k with $k > 1$ (this assumes that the dependence of the oscillation indicators $\beta_l(\cdot)$ on v cannot be reduced to a direct dependence on higher order differences $\Delta^k v$). For the median-interpolating scheme of Example 2, a close look at

the coefficient representations reveals that offset invariance can hold only for \mathbf{P}_1 but polynomial reproduction of order at least $k = 2$ holds. For the power- p scheme, both definitions apply for $k = 2$.

As all our examples indicate, offset invariance for \mathbf{P}_k of a nonlinear scheme is to be expected to hold for $k = 1$, sometimes holds with $k = 2$ but no nonlinear examples of relevance are known for larger k . However, it is the right concept for the extension of the notion of *derived subdivision operators* to the nonlinear setting.

Theorem 1. *Let S be a local, r -shift invariant subdivision operator. If S is offset invariant for \mathbf{P}_k for some integer $k \geq 1$ then there exist local, r -shift invariant derived subdivision operators $S^{[m]} : \ell_p(\mathbb{Z}) \rightarrow \ell_p(\mathbb{Z})$ such that*

$$\Delta^m S v = S^{[m]} \Delta^m v, \quad \forall v \in \ell_p(\mathbb{Z}) \quad (21)$$

for $m = 1, 2, \dots, k$. Moreover, if S is written in the form (16) then its derived subdivision operators $S^{[m]}$, $m = 1, \dots, k$, inherit such a representation with the same (or smaller) L_1, L_2 , and with functions $\phi_s^{[k]}$ that are obtained from the ϕ_s by superpositions involving only linear transformations. In particular, if S (and thus the functions $\phi_s(\cdot)$) is bounded (continuous, Lipschitz continuous, C^1, \dots) then so is $S^{[k]}$ (and the functions $\phi_s^{[k]}$). In particular, if S is bounded then

$$\|S^{[m]} w\|_{\ell_p(\mathbb{Z})} \leq r^{-m+1/p} \|w\|_{\ell_p(\mathbb{Z})} + C \|\Delta w\|_{\ell_p(\mathbb{Z})}, \quad (22)$$

and if S is Lipschitz continuous then

$$\|S^{[m]} w - S^{[m]} w'\|_{\ell_p(\mathbb{Z})} \leq r^{-m+1/p} \|w - w'\|_{\ell_p(\mathbb{Z})} + C \|\Delta(w - w')\|_{\ell_p(\mathbb{Z})}, \quad (23)$$

$m = 0, 1, \dots, k-1$, with constants C independent of $w, w' \in \ell_p(\mathbb{Z})$.

The proof extends the standard argument for linear S , see [10, 26]. For $k = 1$ it was first given in [64, Theorem 2.5], see also [36, Lemma 2.1-2]. The case $k > 1$ was suggested in [36, Section 2.1] and can be obtained by induction from $k = 1$.

Definition 2 can be replaced by a recursive one: S is offset invariant for $k \geq 2$ if it is offset invariant for \mathbf{P}_{k-1} , and the scaled version of the associated $(k-1)$ -st derived operator $\tilde{S}^{[k-1]} = r^{k-1} S^{[k-1]}$ is offset invariant for constants. If S has polynomial reproduction of order k , then all linear subdivision operators S_v are offset invariant for \mathbf{P}_k , and thus derived subdivision operators $(S_v)^{[m]}$ exist for all $m = 1, \dots, k$ and v . Thus, Theorem 1 covers this case as well. To give a concrete example, let us consider Example 5. We already mentioned that the power- p scheme is offset invariant for \mathbf{P}_2 which follows from observing that $H_p((\Delta^2(v+q|z))_{i-1}, (\Delta^2(v+q|z))_i) = H_p((\Delta^2 v)_{i-1}, (\Delta^2 v)_i)$ for all $v, i \in \mathbb{Z}$, and $q \in \mathbf{P}_2$. From (14) we find

$$(\Delta S v)_{2i} = \frac{\Delta v_i}{2} - \frac{1}{8} H_p(\Delta^2 v_{i-1}, \Delta^2 v_i), \quad (\Delta S v)_{2i+1} = \frac{\Delta v_i}{2} + \frac{1}{8} H_p(\Delta^2 v_{i-1}, \Delta^2 v_i),$$

and

$$\begin{aligned} (\Delta^2 S v)_{2i} &= \frac{1}{4} H_p(\Delta^2 v_{i-1}, \Delta^2 v_i), \\ (\Delta^2 S v)_{2i+1} &= \frac{\Delta^2 v_i}{2} - \frac{1}{8} (H_p(\Delta^2 v_{i-1}, \Delta^2 v_i) + H_p(\Delta^2 v_i, \Delta^2 v_{i+1})), \end{aligned} \quad i \in \mathbb{Z}.$$

Thus, the derived subdivision operators $S^{[1]}$ and $S^{[2]}$ are given by

$$\begin{aligned} (S^{[1]} w)_{2i} &= \frac{w_i}{2} - \frac{1}{8} H_p(\Delta w_{i-1}, \Delta w_i), \\ (S^{[1]} w)_{2i+1} &= \frac{w_i}{2} + \frac{1}{8} H_p(\Delta w_{i-1}, \Delta w_i), \\ (S^{[2]} w)_{2i} &= \frac{1}{4} H_p(w_{i-1}, w_i), \\ (S^{[2]} w)_{2i+1} &= \frac{w_i}{2} - \frac{1}{8} (H_p(w_{i-1}, w_i) + H_p(w_i, w_{i+1})), \end{aligned} \quad i \in \mathbb{Z}. \quad (24)$$

2.3 Convergence and Smoothness

In the univariate case, L_p -convergence of the reconstruction part

$$v^j = S v^{j-1} + P d^j, \quad j \geq 1, \quad (25)$$

of a multi-scale transform resp. the subdivision scheme

$$v^j = S v^{j-1}, \quad j \geq 1, \quad (26)$$

associated with it to a limit function, and the smoothness of the latter, can be studied by associating with v^j its linear spline interpolants f^j on the grid $\Gamma^j = r^{-j} \mathbb{Z}$:

$$f^j(x) = (i+1 - r^j x) v_i^j + (r^j x - i) v_{i+1}^j, \quad x \in [r^{-j} i, r^{-j} (i+1)), \quad i \in \mathbb{Z}. \quad (27)$$

Alternatively, we can write $f^j = \sum_i v_i^j B_2(r^j \cdot - i)$ using linear B-splines (with $B_2(x) = 1 - |x|$ for $|x| \leq 1$, and $B_2(x) = 0$ otherwise), and think of f^j as the limit of a linear subdivision process for B-splines of order 2.

Definition 3. The multi-scale reconstruction algorithm (25) is called L_p convergent if, for any $v^0 \in \ell_p(\mathbb{Z})$ and detail sequences $d^j \in \ell_p(\mathbb{Z})$ satisfying

$$\sum_{j \geq 1} r^{-j/p} \|d^j\|_{\ell_p(\mathbb{Z})} < \infty, \quad (28)$$

the corresponding sequence of linear interpolants f^j converges in $L^p(\mathbb{R})$ to a limit function $f^\infty \in L_p(\mathbb{R})$.

Similarly, if the subdivision scheme (26) associated with S is called L_p convergent if $f^j \rightarrow f^\infty \neq 0$ in $L_p(\mathbb{R})$ for any $v^0 \neq \mathbf{0}$.

In applications to multi-scale solvers for operator equations [15, 12] and geometric modeling [26] the smoothness characteristics and sometimes also shape properties of the limits f^∞ matter. Smoothness of functions that are limits of approximation processes (in our case the recursively constructed sequences $\{f^j\}$ of linear splines) is conveniently measured in the scale of Besov spaces (see [49] for various equiv-

alent definitions including the standard one based on moduli of smoothness). We give a definition for a subclass of Besov spaces using an approximation-theoretic characterization which is convenient for our setup. Let $1 \leq p \leq \infty$, $k = 1, 2, \dots$, and $0 < s < k - 1 + 1/p$. A function $f \in L_p(\mathbf{R})$ belongs to the Besov space $B_p^s(\mathbf{R})$ if and only if there exists at least one L_p convergent series representation

$$f = \sum_{j=0}^{\infty} h^j,$$

where the functions h^j are splines of order k with knots at the grid points $\Gamma^j = r^{-j}\mathbf{Z}$, satisfying the constraint

$$\sum_{j=0}^{\infty} r^{sj} \|h^j\|_{L_p(\mathbf{R})}^p < \infty,$$

if $1 \leq p < \infty$, and

$$\sup_{j \geq 0} r^{sj} \|h^j\|_{L_\infty(\mathbf{R})} < \infty,$$

if $p = \infty$. Moreover, we can define a norm in $B_p^s(\mathbf{R})$ by setting

$$\|f\|_{B_p^s(\mathbf{R})} := \begin{cases} \inf \left(\sum_{j=0}^{\infty} r^{sj} \|h^j\|_{L_p(\mathbf{R})}^p \right)^{1/p}, & 1 \leq p < \infty, \\ \inf \sup_{j \geq 0} r^{sj} \|h^j\|_{L_\infty(\mathbf{R})}, & p = \infty, \end{cases} \quad (29)$$

where the infimum is taken with respect to all such representations. For given s , the choice of k is secondary: Norms for different k are equivalent (for this reason, we did not show the dependence of the Besov space norm on k). Proofs based on Jackson-Bernstein inequalities for splines and references can be found in [11, 50, 15]. Note that for the two important subcases $p = \infty$ and $p = 2$, the scale $B_p^s(\mathbf{R})$, $s > 0$, coincides with the scale of Hölder-Zygmund classes \mathcal{C}^s resp. Sobolev spaces $H^s(\mathbf{R}) = W_2^s(\mathbf{R})$.

We are now ready to discuss the smoothness of the algorithms (25) and (26)

Definition 4. The subdivision scheme (26) associated with S possesses L_p smoothness $s > 0$ if it is L_p convergent, with limit functions satisfying

$$f^\infty \in B_p^{s-}(\mathbf{R}) := \bigcup_{0 < t < s} B_p^t(\mathbf{R}), \quad \forall v^0 \in \ell_p(\mathbf{Z}).$$

The maximal such $s > 0$ is called the L_p smoothness exponent of S , and denoted by $s_p(S)$.

The following theorem is proved in [13, 49] for S of the form (19).

Theorem 2. Let S be a local, r -shift invariant, bounded subdivision operator in $\ell_p(\mathbf{Z})$, represented by (19) via a family of linear subdivision operators $\{S_v, v \in \ell_p(\mathbf{Z})\}$ which are uniformly bounded,

$$\|S_v w\|_{\ell_p(\mathbf{Z})} \leq C \|w\|_{\ell_p(\mathbf{Z})}, \quad \forall w, v \in \ell_p(\mathbf{Z}),$$

and have polynomial reproduction order k for some integer $k \geq 1$. Let P be a bounded operator on $\ell_p(\mathbb{Z})$.

i) If

$$\rho_{p,k}(\{S_v\}) := \limsup_{j \rightarrow \infty} \sup_{v^0 \in \ell_p(\mathbb{Z})} \|(S_{v^{j-1}})^{[k]} \dots (S_{v^1})^{[k]} (S_{v^0})^{[k]}\|_{\ell_p(\mathbb{Z}) \rightarrow \ell_p(\mathbb{Z})}^{1/j} < r^{1/p}, \quad (30)$$

then S is L_p convergent. In this case, a lower bound for the L_p smoothness exponent of S is given by

$$s_p(S) \geq \min(k, -\log_r(r^{-1/p} \rho_{p,k}(\{S_v\}))) > 0. \quad (31)$$

ii) If

$$\tilde{\rho}_{p,k}(\{S_v\}) := \limsup_{j \rightarrow \infty} \sup_{w^l \in \ell_p(\mathbb{Z}), l=0, \dots, j-1} \|(S_{w^{j-1}})^{[k]} \dots (S_{w^1})^{[k]} (S_{w^0})^{[k]}\|_{\ell_p(\mathbb{Z}) \rightarrow \ell_p(\mathbb{Z})}^{1/j}, \quad (32)$$

satisfies $\tilde{\rho}_{p,k}(\{S_v\}) < r^{1/p}$, then the multi-scale reconstruction algorithm (25) is L_p convergent.

Moreover, if for some s satisfying

$$0 < s < \min(k, -\log_r(r^{-1/p} \rho_{p,k}(\{S_v\})))$$

the norm

$$\|\{v^0, d^j\}_{j \geq 1}\|_{p,s,r} := \begin{cases} \left(\|v^0\|_{\ell_p(\mathbb{Z})}^p + \sum_{j \geq 1} r^{j(sp-1)} \|d^j\|_{\ell_p(\mathbb{Z})}^p \right)^{1/p}, & 1 \leq p < \infty, \\ \sup\{\|v^0\|_{\ell_p(\mathbb{Z})}, r^{j(s-1/p)} \|d^j\|_{\ell_p(\mathbb{Z})}\}_{j \geq 1}, & p = \infty. \end{cases}$$

is finite, then the limit function f of the multi-scale reconstruction (25) belongs to $B_p^s(\mathbb{R})$, and

$$\|f\|_{B_p^s(\mathbb{R})} \leq C \|\{v^0, d^j\}_{j \geq 1}\|_{p,s,r}. \quad (33)$$

The counterpart of this theorem for S that are offset invariant for \mathbf{P}_k and thus possess derived subdivision operators $S^{[l]}$, $l = 1, \dots, k$, is formulated in the next theorem. In this generality it is new, although partial cases have appeared before, see, e.g., [2] for $p = \infty$.

Theorem 3. Let S be a local, r -shift invariant, bounded subdivision operator operator on $\ell_p(\mathbb{Z})$. Assume that S is offset invariant for \mathbf{P}_k for some integer $k \geq 1$.

i) If

$$\rho_{p,k}(S) = \rho_p(S^{[k]}) := \limsup_{j \rightarrow \infty} \|(S^{[k]})^j\|_{\ell_p(\mathbb{Z}) \rightarrow \ell_p(\mathbb{Z})}^{1/j} < r^{1/p} \quad (34)$$

then S is L_p convergent, and

$$s_p(S) \geq \min(k, -\log_r(r^{-1/p} \rho_{p,k}(S))) > 0. \quad (35)$$

ii) If, in addition, S is Lipschitz continuous, and P is bounded, then (34) also implies the L_p convergence of the multi-scale reconstruction (25). Moreover, if for some s satisfying $0 < s < \min(k, -\log_r(r^{-1/p}\rho_{p,k}(S)))$ we have

$$\|\{v^0, d^j\}_{j \geq 1}\|_{p,s;r} < \infty,$$

then the limit function f belongs to $B_p^s(\mathbf{R})$ and (33) holds.

A couple of comments on the introduced spectral radii, and the range of applicability of the two theorems are in order. First of all, instead of \limsup one can write \lim in all three cases. Also, by definition $\tilde{\rho}_{p,k}(\{S_v\}) \geq \rho_{p,k}(\{S_v\})$. Secondly, by the definition of derived subdivision operators, both $\rho_{p,k}(\{S_v\})$ and $\rho_{p,k}(S) = \rho_p(S^{[k]})$ are tied to geometric decay estimates for the norms of the sequences $\Delta^k v^j$, where $v^j = S v^{j-1} = S^j v^0$. E.g., by repeatedly applying

$$\Delta^k v^j = \Delta^k S_{v^{j-1}} v^{j-1} = (S_{v^{j-1}})^{[k]} \Delta^k v^{j-1},$$

for the subdivision algorithm (26), we have

$$\begin{aligned} \|\Delta^k v^j\|_{\ell_p(\mathbf{Z})} &\leq \|(S_{v^{j-1}})^{[k]} \dots (S_{v^1})^{[k]} (S_{v^0})^{[k]}\|_{\ell_p(\mathbf{Z}) \rightarrow \ell_p(\mathbf{Z})} \|\Delta^k v^0\|_{\ell_p(\mathbf{Z})} \\ &\leq C \rho^j \|\Delta^k v^0\|_{\ell_p(\mathbf{Z})} \end{aligned}$$

for $j \geq 1$, whenever $\rho > \rho_{p,k}(\{S_v\})$. The constant C only depends on k and the chosen ρ .

The same argument goes through for $\rho_{p,k}(S)$. However, in this case the infimum of the set of all ρ for which such a geometric decay holds equals $\rho_{p,k}(S)$. To see this, observe that $\Delta^k v^j = (S^{[k]})^j \Delta^k v^0$ for all v_0 , and thus

$$\|(S^{[k]})^j\|_{\ell_p(\mathbf{Z}) \rightarrow \ell_p(\mathbf{Z})} = \rho_{p,k;j}(S) := \sup_{\|\Delta^k v\|_{\ell_p(\mathbf{Z})}=1} \|\Delta^k S^j v\|_{\ell_p(\mathbf{Z})}, \quad (36)$$

and

$$\rho_{p,k}(S) = \limsup_{j \rightarrow \infty} \rho_{p,k;j}(S)^{1/j} = \inf\{\rho : \|\Delta^k S^j v\|_{\ell_p(\mathbf{Z})} \leq C \rho^j \|\Delta^k v\|_{\ell_p(\mathbf{Z})}\}. \quad (37)$$

By definition of derived subdivision operators of S and the linear operators $\{S_v\}$ we have $(S_v)^{[k]} \Delta^k v = \Delta^k S_{v,v} = \Delta^k S v = S^{[k]} \Delta^k v$, consequently always

$$\tilde{\rho}_{p,k}(\{S_v\}) \geq \rho_{p,k}(\{S_v\}) \geq \rho_{p,k}(S), \quad (38)$$

if the conditions for the existence of these spectral radii are met. (38) holds for all admissible choices of the family of linear subdivision operators $\{S_v\}$ representing S . Since in practice offset invariance for \mathbf{P}_k holds often with $k \leq 2$ only, part a) of Theorem 2 offers sometimes greater flexibility because it may even apply for larger k . A concrete example is given by the dyadic median-interpolating subdivision scheme [52] for which offset invariance for \mathbf{P}_k holds for $k = 1$ only, and

$\rho_{p,1}(S) = 1/2$, while $\{S_v\}$ in the representation (19) have polynomial reproduction of order $k = 2$ and $\rho_{p,2}(\{S_v\}) < 1/2$. The dyadic median-interpolating subdivision scheme also provides an instance when the first inequality in (38) is strict, see [52]. A comparison of $\tilde{\rho}_{p,k}(\{S_v\})$ and $\rho_{p,k}(S)$ is more subtle since S does not define $\{S_v\}$ uniquely. An example of an operator S showing that $\tilde{\rho}_{p,k}(\{S_v\}) > \rho_{p,k}(S)$ for *any* admissible choice of the family $\{S_v\}$ is, to the best of our knowledge, not known. The additional assumption of Lipschitz stability for part b) of Theorem 2 represents a mild restriction since most schemes satisfy it (the exception is the ENO scheme). Moreover, Lipschitz stability of S is necessary for the stability of subdivision and multi-scale reconstruction algorithms associated with S , a desirable property which is discussed in the next subsection.

Another useful property of the spectral radii is that

$$\rho_{p,m}(S) \leq \max(r^{-m+1/p}, \rho_{p,k}(S)), \quad m = 1, \dots, k-1, \quad (39)$$

and similar inequalities hold for $\rho_{p,m}(\{S_v\})$ and $\tilde{\rho}_{p,m}(\{S_v\})$. For the proof it is enough to consider $m = k-1$, the rest follows by recursion. Set $\hat{\rho} = r^{-k+1+1/p}$, and $w = (S^{[k-1]})^{n-1}v$ in (22). Then

$$\begin{aligned} \|(S^{[k-1]})^n v\|_{\ell_p(\mathbf{Z})} &\leq \hat{\rho} \|(S^{[k-1]})^{n-1} v\|_{\ell_p(\mathbf{Z})} + C \|\Delta (S^{[k-1]})^{n-1} v\|_{\ell_p(\mathbf{Z})} \\ &= \hat{\rho} \|(S^{[k-1]})^{n-1} v\|_{\ell_p(\mathbf{Z})} + C \|(S^{[k]})^{n-1} \Delta v\|_{\ell_p(\mathbf{Z})} \\ &\leq \hat{\rho} \|(S^{[k-1]})^{n-1} v\|_{\ell_p(\mathbf{Z})} + C \rho^n \|v\|_{\ell_p(\mathbf{Z})}, \end{aligned}$$

where $\rho = \rho_{p,k}(S) + \varepsilon$ is fixed with arbitrary $\varepsilon > 0$. By recursion,

$$\|(S^{[k-1]})^n v\|_{\ell_p(\mathbf{Z})} \leq C \|v\|_{\ell_p(\mathbf{Z})} \sum_{i=0}^n \hat{\rho}^{n-i} \rho^i \leq C n (\max(\hat{\rho}, \rho))^n \|v\|_{\ell_p(\mathbf{Z})}.$$

This shows that $\rho_{p,k-1}(S) \leq \max(\hat{\rho}, \rho)$, and (39) follows if $\varepsilon \rightarrow 0$.

In applications, to get upper bounds for the above spectral radii, estimates for the quantities $\rho_{p,k;j}(S)$ defined in (36) are used for small values of j . Unfortunately, as experimental evidence shows, the convergence of $\rho_{p,k;j}(S)^{1/j}$ towards $\rho_{p,k}(S)$ is generally very slow. Alternatively, due to the locality of the subdivision operators involved, $\rho_{p,k}(S)$ can also be characterized as the ℓ_p -joint spectral radius of a certain family of nonlinear maps acting on a certain \mathbb{R}^M , where M depends on the dilation factor r and the support length L of S . For linear subdivision operators S , there is an extensive literature on this subject, especially for the cases $p = 2$ and $p = \infty$. In the nonlinear case there is much room for further research.

As an illustration, let us consider the power p -scheme (Example 5). As was mentioned in subsection 2.1, the associated subdivision operator is offset invariant for \mathbf{P}_k , $k = 1, 2$, with explicit formulas for $S^{[k]}$ given in (24). The limiter $H_p(x, y)$ from (15) vanishes whenever $xy \leq 0$ and otherwise satisfies

$$0 < \alpha(x, y) := \frac{2H_p(x, y)}{x + y} \leq 1, \quad xy > 0.$$

Thus, setting $\alpha(x, y) = 0$ for $xy \leq 0$, and denoting $\alpha_i := \alpha(w_{i-1}, w_i)$, we easily get from (24) that

$$\begin{aligned} (S^{[2]}w)_{2i} &= \frac{\alpha_i}{8}(w_{i-1} + w_i), \\ (S^{[2]}w)_{2i+1} &= \frac{1}{16}((8 - \alpha_i - \alpha_{i+1})w_i - \alpha_i w_{i-1} - \alpha_{i+1} w_{i+1}). \end{aligned}$$

Taking absolute values, we immediately get

$$|(S^{[2]}w)_{2i}| \leq \frac{1}{4} \max\{|w_{i-1}|, |w_i|\}, \quad |(S^{[2]}w)_{2i+1}| \leq \frac{1}{2} \max\{|w_{i-1}|, |w_i|, |w_{i+1}|\},$$

which, according to (36) for $j = 1$, gives

$$\rho_{\infty,2}(S) \leq \|S^{[2]}\|_{\ell_{\infty}(\mathbf{Z}) \rightarrow \ell_{\infty}(\mathbf{Z})} \leq \frac{1}{2} < 1.$$

Thus, this crude estimate implies uniform convergence, and gives $s_{\infty}(S) \geq 1$ for any power- p subdivision scheme. In this particular case, this estimate for the Hölder exponent is sharp: For the initial sequence $v^0 = (\dots, 0, 1, 0, 1, \dots)$, the limit f^{∞} is the linear spline interpolant to these data on \mathbb{Z} , and does not belong to $C^1(\mathbb{R})$, and thus to any $B_{\infty}^s(\mathbb{R})$ with $s > 1$. The final result for the Hölder exponent of these schemes is $s_{\infty}(S) = 1$ which is known for a long time (for $p = 2$, see [29], for other p , see, e.g., [2]). We conjecture that

$$s_q(S) = -\log_2(\rho_{q,2}(S)) + \frac{1}{q} = 1 + \frac{1}{q}, \quad 1 \leq q < \infty, \quad (40)$$

holds for all power- p schemes but have verified this only in partial situations such as for the convexity-preserving case $p \leq 2$, where

$$\|S^{[2]}w\|_{\ell_q(\mathbf{Z}) \rightarrow \ell_q(\mathbf{Z})} = \frac{1}{2}, \quad 1 \leq q \leq \infty,$$

can be deduced from the already established result for $q = \infty$ and from the case $q = 1$ by complex interpolation (the upper bound $s_q(S) \leq 1 + 1/q$ follows from the same linear spline example as used for $q = \infty$).

However, in most examples of nonlinear S , the trivial upper estimates

$$\rho_{q,k}(\{S_v\}) \leq \sup_v \|(S_v)^{[k]}\|_{\ell_q(\mathbf{Z}) \rightarrow \ell_q(\mathbf{Z})}$$

resp.

$$\rho_{q,k}(S) \leq \|S^{[k]}\|_{\ell_q(\mathbf{Z}) \rightarrow \ell_q(\mathbf{Z})}$$

for the spectral radii are just too weak (in this regard, the power- p schemes represent an exception), and one needs to resort to (36) for $j > 1$ to obtain more rigorous bounds.

The computation of exact values for these spectral radii and for the smoothness exponents $s_q(S)$ becomes a subtle issue. In this respect the nonlinear case is much harder than the case of linear subdivision operators S , where it can be reduced to the q -joint spectral radius problem for finite families of matrices, or in the special case of L_2 -smoothness exponents to a finite dimensional eigenvalue problem, see, e.g., [40, 68]. Finding the smoothness exponents of nonlinear schemes usually means to enter a detailed study of the nonlinear dynamics hidden in the subdivision scheme.

The only nontrivial case, where such an investigation has led to success is the paper [64] by Xie and Yu, where

$$s_\infty(S) = 1$$

has been established for the triadic median-interpolating S (Example 2). The same authors [64, 63] have also propagated a conjecture on *smoothness equivalence*: For many nonlinear S , the smoothness exponent $s_q(S)$ coincides with the smoothness exponent of a near-by linear S_0 . Currently this conjecture is established only in a few cases, in particular for manifold-valued subdivision schemes [65]. For the power- p subdivision operator S , the appropriate S_0 is equivalent to linear B-spline subdivision, and obtained if the limiter term $H_p(\cdot)$ is dropped from the definition. For median-interpolating schemes, S_0 is given by systematically replacing all conditions of median interpolation by interpolation conditions at the interval midpoints, more examples can be found in [65].

2.4 Stability

Stability of multi-scale transforms, i.e., the robustness with respect to small perturbations, is not a major issue for linear schemes since convergence of a linear subdivision scheme implies stability. However, for nonlinear schemes it is by no means obvious, and deserves consideration. In this paragraph, we consider only the case of Lipschitz stability in $L_p(\mathbb{R})$. We will again deal with the simplified version (9) of a nonlinear multi-scale transform, and its parts: The reconstruction part (25), the associated subdivision scheme (26), and the decomposition part

$$v^{j-1} = Rv^j, \quad d^j = D(v^j - Sv^{j-1}), \quad j = J, J-1, \dots, 1. \quad (41)$$

Definition 5. The decomposition algorithm (41) is called L_p stable if there is a constant C_D such that

$$\max\{\|v^0 - \tilde{v}^0\|_{\ell_p(\mathbb{Z})}, r^{-j/p} \|d^j - \tilde{d}^j\|_{\ell_p(\mathbb{Z})}\}_{j=1, \dots, J} \leq C_D r^{-J/p} \|v^J - \tilde{v}^J\|_{\ell_p(\mathbb{Z})}$$

holds for all $v^J, \tilde{v}^J \in \ell_p(\mathbb{Z})$, and $J \geq 1$.

The reconstruction algorithm (25) is called L_p stable if there is a constant C_U such that

$$r^{-J/p} \|v^J - \tilde{v}^J\|_{\ell_p(\mathbf{Z})} \leq C_U (\|v^0 - \tilde{v}^0\|_{\ell_p(\mathbf{Z})} + \sum_{j=1}^J r^{-j/p} \|d^j - \tilde{d}^j\|_{\ell_p(\mathbf{Z})})$$

holds for all $v^0, \tilde{v}^0 \in \ell_p(\mathbf{Z})$, and $J \geq 1$.

The subdivision algorithm (26) is called L_p stable if there is a constant C_S such that

$$r^{-J/p} \|v^J - \tilde{v}^J\|_{\ell_p(\mathbf{Z})} \leq C_S \|v^0 - \tilde{v}^0\|_{\ell_p(\mathbf{Z})}$$

holds for all $v^0, \tilde{v}^0 \in \ell_p(\mathbf{Z})$, and $J \geq 1$.

For all these definitions it is assumed that the associations

$$\begin{aligned} v^J &\longleftrightarrow \{v^0, d^1, \dots, d^J\} \\ \tilde{v}^J &\longleftrightarrow \{\tilde{v}^0, \tilde{d}^1, \dots, \tilde{d}^J\} \end{aligned}$$

are given by the corresponding recursions in (9), where in the subdivision case detail sequences are set to $\mathbf{0}$.

Defining L_p stability in this form is valuable for realistic algorithms, e.g., for compression based on detail thresholding. The inclusion of the fore-factors $r^{-j/p}$ is dictated by the interpretation of the sequences v^j as representations of an L_p limit function on the grids Γ^j . Indeed, assuming L_p convergence of the reconstruction algorithm studied in the previous subsection, the stability of (25) implies

$$\|f^\infty - \tilde{f}^\infty\|_{L_p(\mathbf{Z})} \leq C_U (\|v^0 - \tilde{v}^0\|_{\ell_p(\mathbf{Z})} + \sum_{j=1}^{\infty} r^{-j/p} \|d^j - \tilde{d}^j\|_{\ell_p(\mathbf{Z})})$$

for the L_p limits of the associated sequences $\{f^j\}_{j \geq 0}$ and $\{\tilde{f}^j\}_{j \geq 0}$. Finally, we note that L_p stability of the decomposition part in a stronger form (e.g., symmetric with the stability condition for (25)) is probably too much to ask for.

We will briefly deal with the decomposition part, where L_p stability can often be determined easily. If R is linear then the condition

$$\|R^n\|_{\ell_p(\mathbf{Z}) \rightarrow \ell_p(\mathbf{Z})} \leq C r^{-n/p}, \quad n \geq 1, \quad (42)$$

together with the Lipschitz continuity of D and S , is a necessary and sufficient condition for the L_p stability of (41). For the nonlinear case the corresponding sufficient condition on R reads

$$\|R^n v - R^n \tilde{v}\|_{\ell_p(\mathbf{Z})} \leq C r^{-n/p} \|v - \tilde{v}\|_{\ell_p(\mathbf{Z})}, \quad n \geq 1,$$

uniformly in v, \tilde{v} , and $n \geq 1$. Indeed, by rephrasing this inequality we get

$$r^{-j/p} \|v^j - \tilde{v}^j\|_{\ell_p(\mathbf{Z})} = r^{-j/p} \|R^{J-j} v^J - R^{J-j} \tilde{v}^J\|_{\ell_p(\mathbf{Z})} \leq C r^{-J/p} \|v^J - \tilde{v}^J\|_{\ell_p(\mathbf{Z})}.$$

The Lipschitz continuity of D and S yields the stability inequalities for d^j , $j = 1, \dots, J$, as well.

With these definitions, trivial down-sampling given by $(Rv)_i = v_{ri}$ which is typical for interpolatory multi-scale transforms leads to L_p stability in (41) only if $p = \infty$, which is logical since point evaluations on L_p functions are not well-defined. On the other hand, if R is a linear averaging restriction operator given by

$$(Rv)_i = \sum_{l \in \mathbb{Z}} b_l v_{ri+l},$$

where the sequence $\{b_l\}$ is finitely supported, non-negative, and satisfying

$$\sum_{i \in \mathbb{Z}} b_{ri+s} = r^{-1}, \quad s = 0, \dots, r-1,$$

then (41) is L_p stable for all $1 \leq p \leq \infty$. Indeed, since $(Rv)_i$ is a convex combination of entries of v , we get

$$\begin{aligned} \|Rv\|_{\ell_p(\mathbb{Z})}^p &\leq \sum_{i \in \mathbb{Z}} \left| \sum_{l \in \mathbb{Z}} b_l v_{ri+l} \right|^p \leq \sum_{l \in \mathbb{Z}} b_l \sum_{i \in \mathbb{Z}} |v_{ri+l}|^p \\ &= \sum_{s=0}^{r-1} \left(\sum_{i \in \mathbb{Z}} b_{ri+s} \right) \left(\sum_{i \in \mathbb{Z}} |v_{ri+s}|^p \right) = r^{-1} \|v\|_{\ell_p(\mathbb{Z})}^p, \end{aligned}$$

and (42) holds with $C = 1$.

The only example of a decomposition algorithm (41) with a nonlinear R comes from Example 2 (median-interpolating schemes), where $r = 3$, and R is defined via (2). The obvious inequality

$$|\text{med}(a, b, c) - \text{med}(a', b', c')| \leq \max(|a - a'|, |b - b'|, |c - c'|)$$

implies L_∞ stability of this R . The example of the two sequences

$$v_i^j = \begin{cases} 0, & i < (3^j - 1)/2 \\ 1, & i \geq (3^j - 1)/2, \end{cases} \quad \tilde{v}_i^j = \begin{cases} 0, & i \leq (3^j - 1)/2 \\ 1, & i > (3^j - 1)/2, \end{cases} \quad i \in \mathbb{Z},$$

shows that $\|v^j - \tilde{v}^j\|_{\ell_p(\mathbb{Z})} = 1$ for all $j = 0, \dots, J$ and $1 \leq p \leq \infty$. Thus, L_p stability cannot hold if $1 \leq p < \infty$.

General results on the L_p stability of the multi-scale reconstruction (25) and of subdivision schemes (26) for S with the representation (19) are developed in [13, 49] for $1 \leq p \leq \infty$, and more recently for S which is offset invariant and for $p = \infty$ in [36] and [2]. We start with formulating the main result of [13, 49] for our definition of L_p stability (note that these papers deal with the limit case $J \rightarrow \infty$, and consider both the L_p and Besov space settings).

Theorem 4. *In addition to the assumptions of Theorem 2, assume that the family $\{S_v\}$ is Lipschitz continuous as function of $v \in \ell_p(\mathbb{Z})$:*

$$\|S_v - S_w\|_{\ell_p(\mathbb{Z}) \rightarrow \ell_p(\mathbb{Z})} \leq C \|v - w\|_{\ell_p(\mathbb{Z})} \quad \forall w, v \in \ell_p(\mathbb{Z}). \quad (43)$$

If $\tilde{\rho}_{p,k}(\{S_v\}) < 1$ then (25) is L_p stable.

Whether L_p stability holds under the weaker and more natural condition $\tilde{\rho}_{p,k}(\{S_v\}) < r^{1/p}$ is an open question. In [13], L_p stability of point-interpolation and cell-average based WENO subdivision (Example 1) is established using Theorem 4.

However, the condition (43) limits the applicability of Theorem 4, as the natural assumption of Lipschitz continuity of the original S does not automatically carry over to the family $\{S_v\}$. Indeed, (43) fails to hold for many concrete multi-scale transforms. Examples 2 and 5 fall into this category. A stability criterion which circumvents this difficulty and is directly based on S has recently been formulated in [36, 2] for $p = \infty$, and has its roots in earlier case studies for some convexity-preserving schemes such as the power-2 subdivision from Example 5, [45, 5]. We formulate the result from [36], and extend it to the whole range $1 \leq p \leq \infty$. For simplicity, we first state it for $k = 1$.

Theorem 5. *Let S be an r -shift invariant, local, offset invariant for \mathbf{P}_1 , and Lipschitz continuous subdivision operator, and let P be bounded and Lipschitz continuous. Then the existence of a ρ , $0 < \rho < 1$, and an integer $n \geq 1$ such that for any two sets $\{v^0, d^j\}$, $\{\tilde{v}^0, \tilde{d}^j\}$ of multi-scale data we have the inequality*

$$r^{-n/p} \|\Delta(v^n - \tilde{v}^n)\|_{\ell_p(\mathbf{Z})} \leq \rho \|\Delta(v^0 - \tilde{v}^0)\|_{\ell_p(\mathbf{Z})} + C \sum_{l=1}^n r^{-l/p} \|d^l - \tilde{d}^l\|_{\ell_p(\mathbf{Z})}, \quad (44)$$

implies the L_p stability of the multi-scale reconstruction (25).

If (44) holds in the special case when $v^0, \tilde{v}^0 \in \ell_p(\mathbf{Z})$ are arbitrary but $d^j = \tilde{d}^j = \mathbf{0}$, $j = 1, \dots, n$, then at least the subdivision scheme (26) is L_p stable.

The statement of this theorem carries over to $k > 1$ if an estimate of the form

$$\|Sv - Sw\|_{\ell_p(\mathbf{Z})} \leq r^{1/p} \|v - w\|_{\ell_p(\mathbf{Z})} + C \|\Delta^k(v - w)\|_{\ell_p(\mathbf{Z})} \quad (45)$$

can be established, and if (44) holds with Δ replaced by Δ^k , see [36]. Moreover, in [36] condition (44) is replaced by a spectral radius estimate on the derivatives of the derived subdivision operators. In the next theorem we formulate this result under the simplifying condition, that all functions ϕ_s in the definition (16) of S possess uniformly bounded, continuous partial derivatives, and refer to [36] for the exact conditions of piecewise continuous differentiability under which the statement can be proved. Denote by $D_v S^{[k]}$ the Frechet derivative of $S^{[k]}$ at $v \in \ell_p(\mathbf{Z})$. Due to our simplifying assumption, the linear operator family $D_v S^{[k]} : \ell_p(\mathbf{Z}) \rightarrow \ell_p(\mathbf{Z})$ depends continuously on v . Now define the spectral radii $\rho_{p,k}^{stab}(S) = \rho_p^{stab}(S^{[k]})$ and $\tilde{\rho}_{p,k}^{stab}(S) = \tilde{\rho}_p^{stab}(S^{[k]})$ as follows:

$$\rho_p^{stab}(S^{[k]}) := \limsup_{j \rightarrow \infty} \sup_{w \in \ell_p(\mathbf{Z})} \|DS_{(S^{[k]})^{j-1}w}^{[k]} DS_{(S^{[k]})^{j-2}w}^{[k]} \cdots DS_w^{[k]}\|_{\ell_p(\mathbf{Z}) \rightarrow \ell_p(\mathbf{Z})}^{1/j}, \quad (46)$$

and

$$\tilde{\rho}_p^{stab}(S^{[k]}) := \limsup_{j \rightarrow \infty} \sup_{w^0, w^1, \dots, w^{j-1} \in \ell_p(\mathbf{Z})} \|DS_{w^{j-1}}^{[k]} DS_{w^{j-2}}^{[k]} \cdots DS_{w^0}^{[k]}\|_{\ell_p(\mathbf{Z}) \rightarrow \ell_p(\mathbf{Z})}^{1/j}. \quad (47)$$

Note that in (47) the supremum is taken with respect to an arbitrary collection of w^l , $l = 0, \dots, j-1$, while in (46) it is taken with respect to a single w . Set $w^l = (S^{[k]})^l w$, $l = 0, \dots, j-1$, to see that

$$\rho_{p,k}^{stab}(S) \leq \tilde{\rho}_{p,k}^{stab}(S).$$

As demonstrated in [36] for the dyadic median interpolating scheme, this inequality can be strict. On the other hand, in [33, Lemma 4.2] it was observed that

$$\lim_{n \rightarrow \infty} \tilde{\rho}_p^{stab}((S^{[k]})^n)^{1/n} = \tilde{\rho}_{p,k}^{stab}(S),$$

a property that is used there for establishing approximation results.

Theorem 6. *Let S be an r -shift invariant, local, Lipschitz continuous subdivision operator, and let P be bounded and Lipschitz continuous. In addition, assume that S is offset invariant for \mathbf{P}_k , and that (45) holds.*

i) The multi-scale reconstruction (25) is L_p stable if $\tilde{\rho}_{p,k}^{stab}(S) < r^{1/p}$, and L_p stability fails to hold when $\tilde{\rho}_{p,k}^{stab}(S) > r^{1/p}$.

ii) The subdivision algorithm (26) is L_p stable if $\rho_{p,k}^{stab}(S) < r^{1/p}$ while in the case $\rho_{p,k}^{stab}(S) > r^{1/p}$ it is not.

For the proof and the generalization to certain classes of piecewise-differentiable S , we refer to [36, Section 2.3] in the case $p = \infty$. The extension to $1 \leq p < \infty$ is straightforward. The L_∞ stability of median-interpolating and power- p multi-scale transforms and subdivision schemes is partially resolved in [36] using Theorem 6. For the power-2 scheme (also called PPH scheme) see [45, 5]. In particular, (25) is L_∞ stable for the power- p case if $1 \leq p < \frac{8}{3}$, and fails to be L_∞ stable if $p > 4$. For the stability analysis of certain monotonicity- and convexity-preserving interpolating subdivision schemes introduced in [44, 46], see [35]. More examples of univariate nonlinear multi-scale transforms, e.g., a triadic version of the power- p scheme or a non-interpolatory PPH scheme with smooth limit functions, can be found in [14, 3].

2.5 Approximation Order and Detail Decay

In this section, we study the L_p convergence of nonlinear multi-scale transforms from a different angle. In contrast to section 2.3, where given multi-scale data $\{v^0, d^j\}_{j \geq 1}$ issues such as L_p convergence and Besov regularity of limit functions were our main concern, we now infer properties of $\{v^0, d^j\}_{j \geq 1}$ from properties of f . In more practical terms, let us interpret the decomposition part (41) of the multi-scale transform as a process of taking sampling values of a smooth function f with respect to Γ^j , and collecting them into the "sampling" vectors v^j . This is, we assume $v^j = R_j f$ for a certain sequence of sampling operators $R_j : L_p(\mathbf{R}) \rightarrow \ell_p(\mathbf{Z})$ which also implicitly define R via $R_{j-1} = R R_j$, $j \geq 1$. E.g., for $p = \infty$ and $f \in C(\mathbf{R})$ sampling by function evaluation at Γ^j given by $v_i^j := f(r^{-j}i)$, $i \in \mathbf{Z}$, $j \geq 0$, is often used, and compatible with trivial down-sampling R given by $(Rv^j)_i = v_{ri}^j$. For

sampling L_p functions ($1 \leq p \leq \infty$), often

$$v_i^j = (R_j f)_i := \int_{\mathbf{R}} f(t) r^j \tilde{\phi}(r^j t - i) dt = \int_{\mathbf{R}} f(r^{-j}(x+i)) \tilde{\phi}(x) dx, \quad i \in \mathbf{Z}, \quad j \geq 0,$$

where $\tilde{\phi}(t) \in L_{p/(p-1),loc}(\mathbf{R})$ has compact support and satisfies $\int_{\mathbf{R}} \tilde{\phi}(x) dx = 1$. If we insist on compatibility with (41) with a local R then $\tilde{\phi}$ needs to be refinable,

$$\tilde{\phi}(x) = r \sum_{l \in \mathbf{Z}} b_l \tilde{\phi}(rx - l), \quad (48)$$

with finitely supported coefficient sequence $\{b_l\}$. The restriction operator R has then the form discussed in the beginning of section 2.4. E.g., taking B-splines of order m as $\tilde{\phi}$ is a common choice, if $m = 1$ then the sampling is equivalent with taking averages on dyadic intervals. Note that trivial down-sampling formally results if $\tilde{\phi} = \delta_0$ is the delta-function which satisfies (48) with the coefficients $b_0 = 1$, $b_i = 0$, $i \neq 0$. In the statement below we will silently include locally supported refinable Radon measures for the generation of sampling operators if $p = \infty$.

All sampling procedures discussed in the literature are linear. The question of how to deal with multi-scale transforms with nonlinear R is open. E.g., no natural sampling compatible with the R defined in Example 2 comes to mind. Median sampling on dyadic intervals as R_j is not suitable since $R_{j-1} = RR_j$ is violated, as simple examples show. In the remainder of this subsection, we therefore discuss only linear R_j . We also assume that the sequence f^j of linear splines associated with $v^j = R_j f$ converges to f for any $f \in L_p(\mathbf{R})$. For the above discussed R_j this assumption is easy to check.

We will discuss the following two questions on the multi-scale transform (9). The first question is to give sharp estimates for the resulting sequence $\{v^j, d^j\}_{j \geq 1}$ in terms of the smoothness class f belongs to. These are usually called *direct or Jackson-type estimates*, for f from Besov-Hölder classes this amounts to proving inequalities opposite to (33). Implicitly, this means to characterize the decay of the detail sequences d^j . The second, related question is the *approximation order* of the multi-scale transform which addresses the simpler question of how to relate the sampling information $v^j = R_j f$ directly to f , applying only the subdivision scheme, without having access to the detail sequences d^l with $l > j$. Roughly speaking, we speak of approximation order s if any f of smoothness s can be reconstructed using S within error $O(h^s)$ from its samples with respect to a grid of step-size h .

Definition 6. We say that the multi-scale transform (9) has L_p approximation order $s > 0$ if for any $f \in B_p^s(\mathbf{R})$ and any $j \geq 0$, the reconstruction $f_j^\infty \in L_p(\mathbf{R})$ from the sampling sequence v^j exists, i.e., the linear spline interpolants for the sequence $v^j, S v^j, S^2 v^j, \dots$ with respect to the $\Gamma^j, \Gamma^{j+1}, \Gamma^{j+2}, \dots$ converge to f_j^∞ in $L_p(\mathbf{R})$, and that $f_j^\infty \rightarrow f$ in $L_p(\mathbf{R})$ at rate s :

$$\|f - f_j^\infty\|_{L_p(\mathbf{R})} = O(r^{-js}), \quad j \rightarrow \infty. \quad (49)$$

Checking approximation order is closely related to direct estimates via L_p stability of the multi-scale reconstruction (25). To this end, it is enough to realize that f_j^∞ is the L_p limit of the reconstruction (25) with the "perturbed" data $\{v^0, d^1, \dots, d^j, \mathbf{0}, \mathbf{0}, \dots\}$. Suppose a direct estimate of the form

$$\|\{v^0, d^j\}_{j \geq 1}\|_{p,s;r} \leq C \|f\|_{B_p^s(\mathbf{R})}, \quad \forall f \in B_p^s(\mathbf{R}), \quad (50)$$

has been established. Then $f_j^\infty \in L_p(\mathbf{R})$ is well-defined, and using L_p stability we have

$$\begin{aligned} \|f - f_j^\infty\|_{L_p(\mathbf{R})} &\leq C \sum_{l > j} r^{-l/p} \|d^l\|_{\ell_p(\mathbf{Z})} \\ &\leq Cr^{-js} \left(\sum_{l > j} r^{(sp-1)l} \|d^l\|_{\ell_p(\mathbf{Z})}^p \right)^{1/p} \leq Cr^{-js} \|f\|_{B_p^s(\mathbf{R})}. \end{aligned}$$

In [33], this reduction is observed for $p = \infty$. There it is also shown that, under some minor additional conditions, even stability of the subdivision scheme (26) is sufficient to prove the reduction. The papers [17, 66] address related issues for manifold-valued subdivision. Note that the question of approximation order could also be discussed without reference to the full multi-scale transform (9), just as a property of sampling operators $\{R_j\}$, $j \geq 0$, on the one hand, and the subdivision operator S , on the other. Such an approach could be of interest, when a subdivision scheme is used for reconstruction, and multi-scale decomposition and detail decay are not important.

Thus, for the rest of this subsection we concentrate on direct estimates. Although this is a well-studied subject in the linear case [10, 15], very little is known for nonlinear multi-scale transforms (in particular, no results are known if R is also nonlinear). Some results in this direction can be found in [49, Section 2.1]. The following statement covers most them.

Theorem 7. *Let the sampling operators R_j be given as explained above, where $\tilde{\phi} \in L_{p/(p-1),loc}(\mathbf{R})$ is refinable (48). If the operator SR is bounded and offset exact for \mathbf{P}_k , i.e.,*

$$SR(v + q|_{\mathbf{Z}}) = SRv + q|_{\mathbf{Z}}, \quad \forall q \in \mathbf{P}_k, \quad \forall v \in \ell_p(\mathbf{Z}),$$

and

$$\|d\|_{\ell_p(\mathbf{Z})} \leq C \|Pd\|_{\ell_p(\mathbf{Z})}, \quad \forall v \in \ell_p(\mathbf{Z}),$$

then the multi-scale transform satisfies the Jackson-type estimate (50) for all $0 < s < k$.

Note that the result would extend to $s = k$ if in Definition 6 $B_p^k(\mathbf{R})$ is replaced by $B_{p,\infty}^k(\mathbf{R})$, and also applies to point-evaluation sampling if $p = \infty$. Offset exactness of SR is more restrictive than offset invariance, and does not hold if $\{R_j\}$ and S are arbitrarily paired. If S is given then special efforts could go into constructing R and $\tilde{\phi}$ such that $R_j = RR_{j+1}$ holds, and SR becomes offset exact. If R_j is given by

point evaluation then offset exactness of SR for \mathbf{P}_k can be reduced to polynomial exactness of S for \mathbf{P}_k which yields the more familiar sounding statements in [49].

The proof of Theorem 7 is straightforward with the above assumptions since

$$\|d^j\|_{\ell_p(\mathbf{Z})} \leq C\|Pd^j\|_{\ell_p(\mathbf{Z})} = C\|v^j - SRv^j\|_{\ell_p(\mathbf{Z})}.$$

Now, since SR is local, bounded, and offset exact for \mathbf{P}_k , we proceed with

$$|(v^j - SRv^j)_i|^p = |(v^j - q|_{\mathbf{Z}} - SR(v^j - q|_{\mathbf{Z}}))_i|^p \leq C\|v^j - q|_{\mathbf{Z}}\|_{\ell_p(\{i-K, \dots, i+K\})}^p$$

for arbitrary $q \in \mathbf{P}_k$, with some fixed K depending on the support size of R and S .

But

$$\inf_{q \in \mathbf{P}_k} \|v^j - q|_{\mathbf{Z}}\|_{\ell_p(\{i-K, \dots, i+K\})} \leq C\|\Delta^k v^j\|_{\ell_p(\{i-K, \dots, i+K-k\})},$$

and after substitution we arrive at

$$\|d^j\|_{\ell_p(\mathbf{Z})}^p \leq C \sum_{i \in \mathbf{Z}} \|\Delta^k v^j\|_{\ell_p(\{i-K, \dots, i+K-k\})}^p \leq C\|\Delta^k v^j\|_{\ell_p(\mathbf{Z})}^p.$$

Now recall that $v^j = R_j f$, and therefore

$$(\Delta^k R_j f)_i = \int_{\mathbf{R}} \sum_{l=0}^k \binom{k}{l} f(r^{-j}(x+i+l)) \tilde{\phi}(x) dx,$$

which, after standard estimation steps, gives

$$\|d^j\|_{\ell_p(\mathbf{Z})}^p \leq C \left\| \sum_{l=0}^k \binom{k}{l} f(r^{-j}(\cdot + i+l)) \right\|_{L_p([-K', K'])}^p \| \tilde{\phi} \|_{\ell_p(\mathbf{Z})}^p \leq Cr^j \|\Delta_{r^{-j}}^k f\|_{L_p(\mathbf{R})}^p,$$

where K' depends on the support of $\tilde{\phi}$. This is the classical Jackson-type estimate in terms of moduli of smoothness for the details, and (50) follows from the definition of Besov spaces in terms of the latter. See [49] for the proof under slightly different conditions.

To illustrate the use of Theorem 7, consider again Example 5. The power- p scheme uses trivial down-sampling for R and dilation factor $r = 2$. This is compatible with defining $(R_j f)_i := f(2^{-j}i)$, and we are restricted to applying the L_∞ case of the theorem. Since $\Delta^2 q|_{\mathbf{Z}} = \mathbf{0}$ for any linear polynomial q it is easy to check that SR is offset exact for \mathbf{P}_2 . Thus, $f \in B_\infty^s(\mathbf{R})$ implies the estimate

$$\|d^j\|_{\ell_\infty(\mathbf{Z})} \leq C2^{-js} \|f\|_{B_\infty^s(\mathbf{R})}$$

for the decay rate of the detail coefficients resp. the estimate

$$\|f - f_j^\infty\|_{L_\infty(\mathbf{R})} \leq C2^{-js} \|f\|_{B_\infty^s(\mathbf{R})}$$

for the approximation rate for s in the range $0 < s \leq 2$. These estimates cannot be expected to hold for larger s , since power- p schemes reduce to linear interpolation near points of inflection.

3 The Geometric Setting: Case Studies

In this section we consider geometric multi-scale transforms and geometry-based subdivision schemes, again in the univariate case. The prediction operator S appearing in these schemes is also termed as a refinement step, and we present several new such refinement steps. In contrast to the functional setting, geometric schemes operate on vector data (vertex points, edge, and normal vectors of polygonal lines) in a way that prevents us from analyzing them componentwise. So far such nonlinear vector subdivision schemes and multi-scale transforms have been investigated in case studies only, and tools for their systematic analysis have yet to be developed.

In subsection 3.1, we deal with the issue of convergence of few examples of curve subdivision schemes, defined by geometry-based refinement steps, and discuss properties of the limits generated by the schemes. Subsection 3.2 is devoted to geometric multi-scale transforms for planar curves based on the idea of normal multiresolution [34, 19, 55] (discussed briefly as the third example in the introduction). We suggest several new multi-scale transforms, mimicking the original normal multiresolution scheme, but with the linear S there replaced by a nonlinear geometry-based refinement rule. These multi-scale transforms have two sources of nonlinearity, the one is the nonlinearity in the prediction, and the other is the inherent nonlinearity in the definition of the details.

3.1 *Geometry-Based Subdivision Schemes*

A geometry-based refinement step depends on all the components of the points involved simultaneously, in contrast to the linear case, where the refinement step is applied separately to each component. Therefore linear subdivision schemes in the geometric setting are analyzed by the tools for linear subdivision schemes in the functional setting. In contrast, the geometry-based subdivision schemes are the nonlinear analogue of linear vector subdivision schemes, with refinement steps defined by operations of matrices on vectors.

3.1.1 **Three types of geometry-based nonlinear 4-point schemes**

In this subsection we present three geometry-based 4-point schemes, all related to the linear 4-point scheme in different ways. The refinement rule of the linear 4-point scheme is

$$(S_w \mathcal{P})_{2i} = P_i, \quad (S_w \mathcal{P})_{2i+1} = -w(P_{i-1} + P_{i+2}) + \left(\frac{1}{2} + w\right)(P_i + P_{i+1}). \quad (51)$$

In the above, \mathcal{P} denotes a control polygon, namely a polygonal line through a sequence of points, denoted by $\{P_i\}$, and w is a fixed tension parameter (to avoid discussions about boundary treatment, assume a closed or bi-infinite control polygon). This refinement rule includes the one of the Deslauriers-Dubuc scheme (1) for $w = \frac{1}{16}$, and the linear B-spline scheme for $w = 0$ as partial cases.

It is well known that the scheme given by (51) has the following attributes:

- It generates “good” curves when applied to control polygons with edges of comparable length.
- It generates curves which become smoother (have greater Hölder exponent of the first derivative), the closer the tension parameter is to $\frac{1}{16}$.
- Starting from an initial control polygon with edges of significantly different length, S_w with a tension parameter around $\frac{1}{16}$, may generate curves with artifacts.

An artifact is a geometric feature of the generated curve which does not exist in the initial control polygon, such as an inflection point or a self-intersection point.

- S_w generates a curve which preserves the shape of an initial control polygon with edges of significantly different length, only for very small values of w . (Recall that the control polygon itself corresponds to the generated curve with zero tension parameter.)

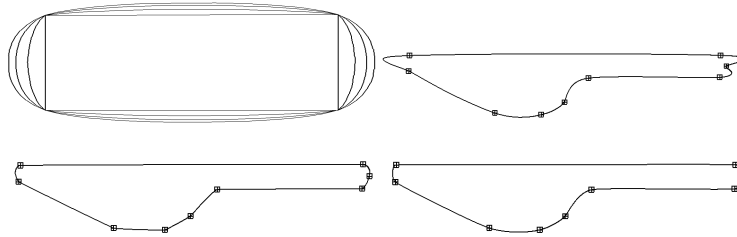


Fig. 5 Curves generated by the linear 4-point scheme: (Upper left) the effect of different tension parameters, (upper right) artifacts in the curve generated with $w = \frac{1}{16}$, (lower left) artifact-free but visually non-smooth curve generated with $w = 0.01$. Artifact-free and visually smooth curve generated in a nonlinear way with adaptive tension parameters (lower right).

Displacement-safe 4-point schemes. This geometry-based version of the 4-point scheme is introduced in [48], and adapts the tension parameter w in (51) to the geometry of the four control points taking part in the definition of an inserted point (a refined point with an odd index). The failure of the 4-point scheme with a fixed tension parameter to generate smooth looking artifact free curves, when the edges

of the initial control polygon are of significantly different length, is demonstrated in Figure 5. Also shown there is a high quality curve generated by a scheme with adaptive tension parameter.

To derive the refinement step with adaptive tension parameter, we write the insertion rule in (51) in terms of the edges $\{e_j = P_{j+1} - P_j\}$ of the control polygon, and relate the inserted point to the edge e_j . The insertion rule can thus be written in the form,

$$(S\mathcal{P})_{2j+1} = P_{e_j} = M_{e_j} + w_{e_j}(e_{j-1} - e_{j+1}) \quad (52)$$

with M_{e_j} the midpoint of e_j , w_{e_j} the adaptive tension parameter, and P_{e_j} the inserted point relative to the edge e_j . Defining $d_{e_j} = w_{e_j}(e_{j-1} - e_{j+1})$ as the displacement from M_{e_j} , we control its size by choosing w_{e_j} according to a geometrical criterion.

In [48] there are various geometrical criteria, all of them guaranteeing that the inserted control point P_{e_j} is different from the boundary points of the edge e_j , and that the length of each of the two edges replacing e_j is bounded by the length of e_j . One way to achieve these goals is to choose w_{e_j} so that

$$\|d_{e_j}\| \leq \frac{1}{2}\|e_j\|. \quad (53)$$

The resulting schemes are termed *displacement-safe*. In all these schemes the value of the tension parameter w_{e_j} is restricted to the interval $(0, \frac{1}{16}]$, such that a tension parameter close to $\frac{1}{16}$ is assigned to *regular stencils*, namely to stencils of four points with three edges of almost equal length, while the *less regular* the stencil is, the closer to zero is the tension parameter assigned to it.

A *natural* choice of an adaptive tension parameter in $(0, \frac{1}{16}]$ obeying (53) is

$$w_{e_j} = \min \left\{ \frac{1}{16}, c \frac{\|e_j\|}{\|e_{j-1} - e_{j+1}\|} \right\}, \quad \text{with a fixed } c \in \left[\frac{1}{8}, \frac{1}{2} \right). \quad (54)$$

In (54), the value of c is restricted to the interval $[\frac{1}{8}, \frac{1}{2})$ to guarantee that $w_{e_j} = \frac{1}{16}$ for stencils with $\|e_{j-1}\| = \|e_j\| = \|e_{j+1}\|$. To see this, observe that in this case, $\|e_{j-1} - e_{j+1}\| = 2 \sin \frac{\theta}{2} \|e_j\|$, with $\theta \in [0, \pi]$ the angle between the two vectors e_{j-1}, e_{j+1} . Thus we have $\|e_j\|/\|e_{j-1} - e_{j+1}\| = (2 \sin \frac{\theta}{2})^{-1} \geq \frac{1}{2}$, and if $c \geq \frac{1}{8}$ then the minimum in (54) is $\frac{1}{16}$. The choice (54) defines irregular stencils (corresponding to small w_{e_j}) as those with $\|e_j\|$ much smaller than at least one of $\|e_{j-1}\|, \|e_{j+1}\|$, and such that when these two edges are of comparable length, the angle between them is not close to zero.

The convergence of this geometric 4-point scheme, and the continuity of the limits generated, follow from a result in [47]. There it is proved that the 4-point scheme with a varying tension parameter is convergent, and that the limits generated are continuous, whenever the tension parameters are restricted to the interval $[0, \tilde{w}]$, with $\tilde{w} < \frac{1}{8}$.

Yet, the result in [47] about C^1 limits of the 4-point scheme with a varying tension parameter does not apply to the geometric 4-point scheme defined by (52) and (54),

since the tension parameters used during this subdivision process are not bounded away from zero.

Nevertheless, many simulations indicate that the curves generated by this scheme are C^1 (see [48]).

Parametrization-based 4-point schemes. This type of schemes is introduced and investigated in [24]. The idea for the geometric insertion rule comes from the insertion rule of the linear scheme with $w = \frac{1}{16}$, corresponding to the Deslaurier-Dubuc 4-point scheme. The point $(S_{1/16}\mathcal{P})_{2i+1}$ is obtained by the evaluation of a cubic polynomial interpolating the data $\{(i-k, P_{i-k}) : k = -1, 0, 1, 2\}$ at the point $i + \frac{1}{2}$ (see [20]). From this point of view, the linear scheme corresponds to a uniform parametrization of the control polygon at each refinement level. This approach fails when the initial control polygon has edges of significantly different length. Yet the use of the centripetal parametrization, instead of the uniform parametrization, leads to a geometric 4-point scheme with artifact-free limit curves, as can be seen in Figure 6.

The centripetal parametrization, which is known to be effective for interpolation of control points by a cubic spline curve (see [28]), has the form $\mathbf{t}_{\text{cen}}(\mathcal{P}) = \{t_i\}$, with

$$t_i = t_{i-1} + \|P_i - P_{i-1}\|_2^{1/2}, \quad (55)$$

where $\|\cdot\|_2$ is the Euclidean norm, and $\mathcal{P} = \{P_i\}$.

Let \mathcal{P}^j be the control polygon at refinement level j , and let $\{t_i^j\} = \mathbf{t}_{\text{cen}}(\mathcal{P}^j)$. The refinement rule for the geometric 4-point scheme, based on the centripetal parametrization is:

$$P_{2i}^{j+1} = P_i^j, \quad P_{2i+1}^{j+1} = \pi_{j,i}\left(\frac{1}{2}(t_i^j + t_{i+1}^j)\right),$$

with $\pi_{j,i}$ the vector of cubic polynomials, satisfying the interpolation conditions

$$\pi_{j,i}(t_{i+k}^j) = P_{i+k}^j, \quad k = -1, 0, 1, 2.$$

Note that this construction can be done with any parametrization. In fact in [24] the chordal parametrization ($t_{i+1} - t_i = \|P_{i+1} - P_i\|_2$) is also investigated, but found to be inferior to the centripetal parametrization (see Figure 6).

The analysis of the schemes in [24] is rather ad-hoc. It is shown there that the centripetal and chordal schemes are well defined, in the sense that any inserted point is different from the end points of the edge to which it corresponds, and that both schemes are convergent to continuous limit curves. Although numerical simulations indicate that both schemes generate C^1 curves, as does the linear 4-point scheme, there is no proof in [24] of such a property for the geometric schemes.

Another type of information on the limit curves, which is relevant to the absence or presence of artifacts, is available in [24]. Bounds on the Hausdorff distance, $d_{\mathcal{H}}$ (see (62)), from sections of a limit curve to their corresponding edges in the initial control polygon are derived. These bounds give a partial qualitative understanding

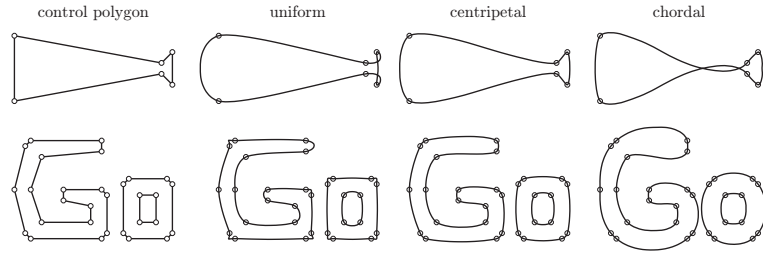


Fig. 6 Comparisons between 4-point schemes based on different parameterizations.

of the empirical observation that the limit curves corresponding to the centripetal parametrization are artifact free.

Let \mathcal{C} denote a curve generated by the scheme based on the centripetal parametrization from an initial control polygon \mathcal{P}^0 . Since the scheme is interpolatory, \mathcal{C} passes through the initial control points. Denote by $\mathcal{C}|_{e_i^0}$ the section of \mathcal{C} with boundary points as those of e_i^0 . Then

$$d_{\mathcal{H}}(\mathcal{C}|_{e_i^0}, e_i^0) \leq \frac{5}{7} \|e_i^0\|_2.$$

Thus the section of the curve corresponding to a short edge cannot be too far from its edge. On the other hand the corresponding bound in the linear case has the form

$$d_{\mathcal{H}}(\mathcal{C}|_{e_i^0}, e_i^0) \leq \frac{3}{13} \max\{\|e_j^0\|_2, |j-i| \leq 2\},$$

and a section of the curve can be rather far from its corresponding short edge, if this edge has a long neighboring edge. In the case of the chordal parametrization the bound is even worse

$$d_{\mathcal{H}}(\mathcal{C}|_{e_i^0}, e_i^0) \leq \frac{11}{5} \max\{\|e_j^0\|_2, |j-i| \leq 2\}.$$

Comparisons of the performance of the three 4-point schemes, based on uniform, chordal and centripetal parametrization, are given in Figure 6.

Circle preserving 4-point scheme. While the first two types of geometric 4-point schemes were designed to alleviate artifacts in the geometry (position) of the limit curves, this geometric version of the 4-point scheme was designed to overcome artifacts in the numerical curvature generated by the linear scheme [57]. The scheme is *circle preserving* in the sense that if the initial control points are ordered points on a circle, then the limit curve is that part of the circle between the first and the last initial control points.

The insertion rule requires geometric computations, as the inserted point is an intersection point between a circle and a sphere. The details of the computation of an inserted point are given in [57] as an algorithm.



Fig. 7 A control polygon and the limit curve generated by the circle preserving variant of the 4-point scheme

Figure 7 from the above paper, demonstrates the limit curve obtained from a control polygon with slowly varying numerical curvature. The numerical curvature of the limit curve is varying smoothly.

It is shown in [57] that the scheme is asymptotically equivalent to the linear 4-point scheme, and therefore according to [25] the scheme is convergent and generates continuous limit curves. Numerical simulations indicate that the scheme generates C^1 limit curves.

The available analysis of the above three types of geometric 4-point schemes, is limited to showing convergence and continuity of the limit curves. The proof of C^1 seems to be much harder due to the lack of an appropriate parametrization for the geometrically defined curves. Perhaps the proof should be in terms of geometric arguments, such as the continuity of the tangents of the curves.

3.1.2 Convexity-preserving schemes in the plane

A shape property of planar control polygons, which is important to have in the curves generated by subdivision, is convexity. Here we present three different subdivision schemes which are convexity preserving in the geometric setting, namely they refine convex polygons into convex polygons.

We first introduce some geometrical notions related to polygonal lines and to convexity.

- An edge in a polygonal line such that its two neighboring edges are in the same half-plane, determined by the line through the edge, is termed a “convex edge”.
- An edge in a polygonal line which is on the same line as one of its neighboring edges is termed a “straight edge”.
- A line through a vertex of a polygonal line, such that the two edges meeting at the vertex are on the same side of the line, is termed a “convex tangent”. A “straight tangent” at a vertex is a line through one of the edges emanating from the vertex.
- A polygonal line consisting of convex and straight edges is termed a “convex polygon”. It is a “strictly convex polygon” if all its edges are convex. In Figure 8 three examples of strictly convex polygons are given.

Among the three convexity preserving schemes presented here, two are nonlinear and geometry-based, while one is linear but of Hermite type. It refines control points

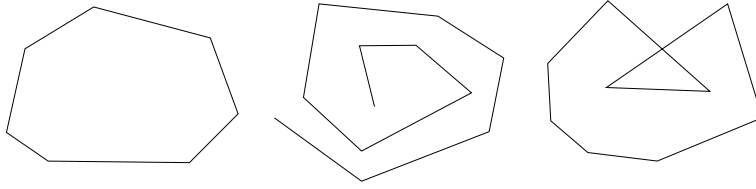


Fig. 8 Convex polygons: (left) closed, (middle) open, (right) self- intersecting.

and normals at the control points, and is inherently related to nonlinear schemes generating surfaces by refining control points and normals.

Convexity preserving 4-point scheme with adaptive tension parameter This scheme is a geometric variant of the 4-point scheme, similar to the displacement-safe schemes, but with the adaptive tension parameter chosen to preserve convexity. It is designed and analyzed in [48]. The scheme refines convex (strictly convex) control polygons into convex (strictly convex) control polygons. We describe the geometrical construction of the inserted points in terms of notation introduced in the first part of subsection 3.1.1.

As a first step in the construction, at each control point from which at least one convex edge emanates, a convex tangent is constructed. At the other control points a straight tangent is constructed, coinciding with one of the straight edges meeting at the control point. We denote the tangent at P_i by t_i .

In case of a straight edge e_i , $P_{e_i} = M_{e_i}$.

In case of a convex edge e_i , the tangents t_i and t_{i+1} together with e_i determine a triangle, T_{e_i} . By construction, the line through e_i separates T_{e_i} from the edges e_{i-1}, e_{i+1} . Thus the half-line starting from M_{e_i} along the direction $e_{i-1} - e_{i+1}$ intersects T_{e_i} . The point P_{e_i} is chosen so that $\|P_{e_i} - M_{e_i}\|/\|e_{i-1} - e_{i+1}\| \leq \frac{1}{16}$ and that $P_{e_i} \in T_{e_i}$.

These two conditions for point insertion guarantee that $0 \leq w_{e_i} \leq \frac{1}{16}$ and that the refined control polygon $S\mathcal{P}$ obtained from \mathcal{P} by the refinement rule

$$(S\mathcal{P})_{2i} = P_i, (S\mathcal{P})_{2i+1} = P_{e_i},$$

is convex (strictly convex) if the control polygon \mathcal{P} is (see [48]).

This construction of refined control polygons, when repeated, generates a sequence of convex (strictly convex) polygons from an initial convex (strictly convex) polygon. It is proved by arguments similar to those cited in subsection 3.1.1 for the displacement-safe schemes, that this sequence converges, and that the limit is a continuous convex (strictly convex) curve. Moreover, it is shown that the curve between two consecutive initial control points is either a line segment when the edge connecting the two points in the initial control polygon is straight, or otherwise a strictly convex curve.

Note that the subdivision scheme is interpolatory and that the inserted point between P_i and P_{i+1} depends on the points $P_{i-1}, P_i, P_{i+1}, P_{i+2}$ as in the linear 4-point scheme.

The convex tangents in this construction can be chosen in different ways. A natural choice of such a tangent is

$$t_i = P_{i+1} - P_{i-1} = e_i + e_{i-1}. \quad (56)$$

This choice was tested in many numerical experiments, and was found superior to other choices.

In Figure 9, the performance of this convexity-preserving scheme is compared on several examples with that of the displacement-safe scheme of subsection 3.1.1 and with that of the linear 4-point scheme.

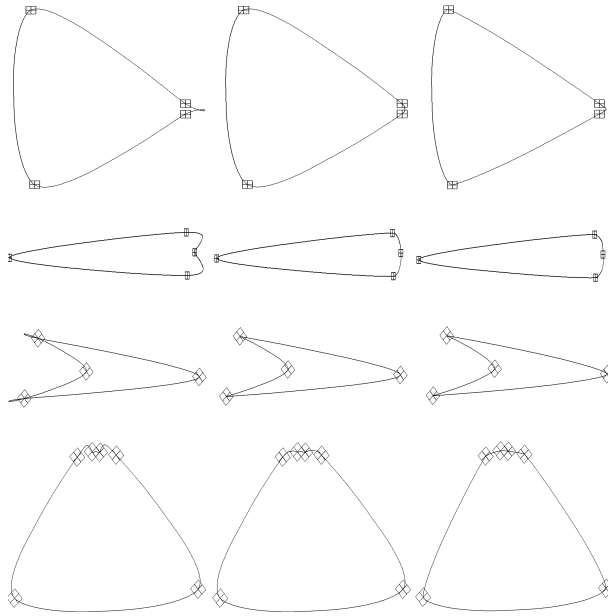


Fig. 9 Examples: (left column) the linear 4-point scheme with $w = 1/16$, (middle column) the displacement-safe scheme of subsection 3.1.1, (right column) the convexity preserving 4-point scheme.

The convexity-preserving 4-point scheme is extended in [48] to a co-convexity preserving scheme for general planar polygons.

Convexity preserving 2-point Hermite-type scheme. This convexity preserving scheme is a two-point interpolatory Hermite-type scheme. It operates on data in \mathbf{R}^2 , consisting of control points and unit normals at the control points. It generates a convex limit curve from an initial convex data, namely a strictly convex control polygon, with compatible normals (compatible with the convexity).

The scheme is presented briefly in [16], as a first step in the construction of a nonlinear Hermite-type scheme for the generation of surfaces, interpolating the initial control points and the unit normals attached to them.

The insertion rule for the point between two consecutive points P_i, P_{i+1} is derived from the quadratic Bézier curve interpolating these two points and the normals at these points. First the mid control point, Q_i , of the quadratic Bézier curve is constructed, as the intersection point of the lines through P_i and P_{i+1} , which are orthogonal to the corresponding normals. The parametric midpoint of the Bézier curve determined by the control points P_i, Q_i, P_{i+1} , is the inserted point. It is given by

$$(S\mathcal{P})_{2i+1} = \frac{1}{4}(P_i + 2Q_i + P_{i+1}). \quad (57)$$

The normal at the refined point is the normal of the Bézier curve at this point, which is orthogonal to the direction $P_{i+1} - P_i$.

By construction the limit curve is a C^1 piecewise quadratic Bézier curve.

Convexity preserving scheme refining lines. This scheme is an extension of the 'dual' Chaikin scheme for lines, proposed by Sabin in [56]. It is an interpolatory scheme, which is used and analyzed in [27], as a first step towards the construction of a convexity preserving interpolatory scheme, operating on convex polyhedra and generating in the limit smooth convex surfaces. This scheme, although an interpolatory scheme refining control points, can be regarded as refining the support lines of the convex control polygon determined by the control points at each refinement level.

Given a strictly convex, closed control polygon \mathcal{P} , the first step in the construction of the inserted points, is the assignment of convex tangents $\{t_j\}$ (e.g. as in (56)) to the control points. Now, t_j, e_j, t_{j+1} determine a triangle T_{e_j} . The refined polygon $S\mathcal{P}$ is strictly convex if the inserted point between P_j and P_{j+1} is any point inside T_{e_j} . The rule for assigning convex tangents to the control points of $S\mathcal{P}$ is to keep the convex tangents at the control points of \mathcal{P} and to choose convex tangents at the inserted points.

Denoting by $\langle \mathcal{P} \rangle$ the closed planar set enclosed by \mathcal{P} , and by \mathcal{Q} the convex polygon generated by the convex tangents to the points of \mathcal{P} , it is easy to verify that

$$\langle \mathcal{P} \rangle \subset \langle S\mathcal{P} \rangle \subset \langle \mathcal{Q} \rangle,$$

Thus repeated refinements, starting from an initial strictly convex, closed polygon, generate a sequence of "increasing" closed convex sets (in the sense of inclusion of sets), which are all contained in the closed convex set $\langle \mathcal{Q} \rangle$. This is sufficient to guarantee the convergence of the sequence of strictly convex, closed polygons to a continuous, closed convex curve. Moreover, it is proved in [27] by geometrical arguments, that the limit curve is C^1 .

3.1.3 Ideas for designing new geometry-based schemes

Here we give three geometric constructions of refinement rules. The corresponding schemes have not been analyzed yet. All the schemes are interpolatory.

Interpolatory 4-point scheme based on circular arc approximation. For the construction of the inserted point between P_i and P_{i+1} , first two auxiliary points are constructed. These points are the mid-points of two circular arcs between P_i and P_{i+1} , one on the unique circular arc through P_i, P_{i+1}, P_{i+2} and the other on the unique circular arc through P_{i-1}, P_i, P_{i+1} . The inserted point is the midpoint of the two auxiliary points. It is a point on the line through M_{e_i} orthogonal to e_i . The resulting scheme is circle preserving by construction.

Interpolatory $2n$ -point scheme based on the centripetal parametrization. This is an extension of the second geometric version of the 4-point scheme, presented in subsection 3.1.1. To determine the inserted point between P_i and P_{i+1} , one first parameterize the $2n$ points P_{i+j} , $j = -n + 1, \dots, n$ according to the centripetal parametrization (see (55)) to obtain the parameter differences $t_{i+j+1} - t_{i+j}$, $j = -n + 1, \dots, n - 1$. Then the interpolating polynomial vector of degree $2n - 1$ to the data (t_{i+j}, P_{i+j}) , $j = -n + 1, \dots, n$, is constructed and evaluated at the point $(t_i + t_{i+1})/2$ to yield the inserted point. This family of schemes is a geometric analogue of the Deslauriers-Dubuc family.

Convexity preserving interpolatory scheme based on quadratic Bézier curves. Given a strictly convex, closed control polygon, a refined strictly convex, closed control polygon is generated, by first assigning a convex tangent to each control point, and then computing the intersection points of consecutive convex tangents. The inserted point between P_i and P_{i+1} is the parametric midpoint (57) of the Bézier quadratic curve, determined by the three control points P_i, Q_i, P_{i+1} , where Q_i is the intersection point of the tangents at P_i and at P_{i+1} .

The rule for assigning convex tangents to the control points of the refined polygon, is to keep those at the 'old' control points, and to choose convex tangents at the inserted control points.

Note that an inserted point depends on four control points; two on each side.

3.2 Geometric Multi-Scale Transforms for Planar Curves

We present here results on geometric multi-scale transforms for continuous curves in the plane, all based on the idea of normal multiresolution, which is discussed briefly in the introduction. We also suggest new geometric constructions for normal multiresolution, which have still to be investigated.

3.2.1 The general structure of normal multiresolutions

Here we present again the main features of the normal multiresolution (NM), which aims at a multi-scale representation of curves in the plane, which can be encoded efficiently. The presentation is somewhat more general than that in Example 3 in

section 1, to allow geometric prediction operators. In the following we assume that the curves are continuous.

Given a planar curve, \mathcal{C} , it is approximated by a sequence of polygonal lines $\{\mathcal{P}^j\}_{j \geq 0}$, where $\mathcal{P}^j = \{P_i^j\}$ with points P_i^j on the curve at refinement level j connected by edges $e_i^j = P_i^j - P_{i-1}^j$. As before, let us assume for simplicity that \mathcal{C} is closed, that \mathcal{P}^j contains $n_j = 2^j n_0$ points periodically enumerated by the index $i \in \mathbb{Z}$.

To obtain \mathcal{P}^{j+1} from \mathcal{P}^j , the points P_i^j are retained and denoted by P_{2i}^{j+1} , i.e., their indices are doubled, and between any two consecutive points $P_{2i}^{j+1}, P_{2(i+1)}^{j+1}$ a point from the curve segment \mathcal{C}_i^j between the points P_i^j and P_{i+1}^j , is inserted with the index $2i+1$. The inserted point is obtained by a two-step procedure. First a prediction step $S^j \mathcal{P}^j$, with S^j an interpolatory prediction/subdivision operator, is performed which results in points $\hat{P}_{2i+1}^{j+1} = (S^j \mathcal{P}^j)_{2i+1}$ near the curve segments \mathcal{C}_i^j . The prediction step is followed by a projection step, which determines a point on \mathcal{C} as an intersection of \mathcal{C} with the line orthogonal to the edge e_i^j through the predicted point $(S^j \mathcal{P}^j)_{2i+1}$ (see Figure 3). We denote this projection operator, acting on the predicted point and mapping it to the curve, by R^j . Note that for general S^j , the resulting point $P_{2i+1}^{j+1} := (R^j S^j \mathcal{P}^j)_{2i+1}$ is not necessarily on \mathcal{C}_i^j . Since the projection operator R^j is determined by the geometry of \mathcal{P}^j and by the points $S^j \mathcal{P}^j$, it is a property of the prediction operator S^j and of \mathcal{P}^j which guarantees that the inserted points are on the correct curve segments. We term a pair $\{S^j, \mathcal{P}^j\}$ *admissible for NM at level j* , if for all i

$$(R^j S^j \mathcal{P}^j)_{2i+1} \in \mathcal{C}_i^j.$$

Thus, if the pair $\{S^j, \mathcal{P}^j\}$ is admissible for NM at level j , then the polygonal line \mathcal{P}^{j+1} consists of the vertices

$$P_{2i}^{j+1} = P_i^j, \quad P_{2i+1}^{j+1} = (R^j S^j \mathcal{P}^j)_{2i+1} \quad (58)$$

in a natural ordering along \mathcal{C} .

In the following we assume that the operators S^j are chosen in advance, e.g., as an insertion rule of an interpolatory linear subdivision scheme, or as an insertion rule of an interpolatory geometric subdivision scheme determined by the geometry of \mathcal{P}^j , so that these operators do not have to be encoded. Moreover we assume that for each $j \geq 0$ the pair $\{S^j, \mathcal{P}^j\}$ is admissible for NM at level j .

Remark: The set of pairs $\{S^j, \mathcal{P}^j\}$ admissible for NM at level j is nonempty. To see this consider the linear mid-point interpolatory subdivision scheme S_0 , with the refinement rule

$$(S_0 \mathcal{P}^j)_{2i} = P_i^j, \quad (S_0 \mathcal{P}^j)_{2i+1} = \frac{1}{2}(P_i^j + P_{i+1}^j), \quad (59)$$

It is easy to verify that any pair $\{S_0, \mathcal{P}^j\}$, with \mathcal{P}^j a polygonal line consisting of vertices sampled from the curve, is admissible for NM at any level. We term a scheme with this property *unconditionally admissible for NM*.

Defining the signed distances from the predicted points $S^j \mathcal{P}^j$ to their corresponding projected points $R^j S^j \mathcal{P}^j$ as *details at level j* , and denoting them by $d^j = \{d_i^j\}$, we observe that these details and the lines connecting pairs of corresponding predicted and projected points, are sufficient for computing the points of \mathcal{P}^{j+1} from \mathcal{P}^j . Since these lines are determined by the information in \mathcal{P}^j , it follows that for the construction of \mathcal{P}^{j+1} from \mathcal{P}^j only the details at level j have to be encoded. Thus, the sequence of polygonal lines $\{\mathcal{P}^j\}_{j=1}^J$ can be reconstructed from the information

$$\mathcal{P}^0, d^1, \dots, d^{J-1}. \quad (60)$$

The gain in the NM is that instead of encoding differences between points, which are vectors, we have to encode signed scalars, and to use the geometric information available at each level for the reconstruction of the next level.

In the following we discuss the case of linear prediction operators.

3.2.2 Normal multiresolutions with linear prediction operators

Denoting by S a linear prediction operator, and considering the stationary case $S^j = S$, equation (58) becomes

$$P_{2i}^{j+1} = P_i^j, \quad P_{2i+1}^{j+1} = (R^j S \mathcal{P}^j)_{2i+1}. \quad (61)$$

It is clear that in this NM the nonlinearity/geometry is introduced by the projection operators R^j .

Note that in the stationary case $S^j = S$, with linear S , the notion *admissible for NM at level j* can be replaced by *admissible for NM*. Moreover for a pair $\{S, \mathcal{P}^0\}$ to start a NM, we need the stronger notion *strongly admissible for NM*, namely that this pair and all the pairs $\{S, \mathcal{P}^j\}$ with $j > 0$ are admissible for NM, where \mathcal{P}^j is the polygonal line generated by j refinement steps of the NM with S , starting from \mathcal{P}^0 .

In [19] NMs with linear subdivision schemes as prediction operators are analyzed. The case of the mid-point prediction operator, given by (59), is easier to analyze and the results are better in some respects. The main issues addressed in [19] are the convergence of the reconstruction and the regularity of the limit, the rate of decay of the details, and the stability of the reconstruction. The rate of decay of the details is strongly related to the quality of the approximation of the curve by the polygonal lines $\{S \mathcal{P}^j\}$. The stability issue is concerned with the effect of small changes in the information (60), on the reconstructed polygons $\{\mathcal{P}^j\}_{j=1}^J$. The NM is termed *stable* if the changes in the reconstructed polygons due to small changes in the information are controlled. In a stable and converging NM, the polygons (and hence the curve) can be well approximated without the small details, allowing a further reduction in the amount of encoded information.

Here we cite several results from [19] on the family of linear 4-point schemes $\{S_w\}$ with $w \in [0, \frac{1}{16}]$, where S_w is given by (51). These schemes constitute the main example in [19]. Note that the scheme S_w with $w = 0$ corresponds to the mid-point

scheme (59), and that the scheme with $w = \frac{1}{16}$ corresponds to the Deslauriers-Dubuc 4-point scheme.

Although the results in [19] are derived in great generality, we limit our presentation to the above family of schemes. This alleviates the need to introduce the rather technical terminology, with which the general results are formulated.

To present the results, we first introduce the notion of the *regularity exponent* of a continuous curve \mathcal{C} with a finite length $\ell(\mathcal{C})$. Let $(x(s), y(s))$, $s \in [0, \ell(\mathcal{C})]$, be a representation of the curve in terms of the arc-length parametrization. The curve has Hölder regularity exponent $\nu = m + \mu$ with m a nonnegative integer and $\mu \in (0, 1]$, if both functions $x(s)$ and $y(s)$ have a continuous m th derivative which is Hölder continuous with exponent greater or equal to μ .

As is observed in subsection 3.2.1, the mid-point scheme S_0 , is unconditionally admissible for NM, and hence can be used as the prediction operator for NM. It is shown in [19] that any member of the family of 4-point schemes $\{S_w\}$ with $w \in (0, \frac{1}{16}]$, can also serve as the prediction operator in NMs of smooth curves. More specifically,

Result 1: Let \mathcal{C} have regularity exponent $\beta > 1$, and let \mathcal{P} be a polygonal line with vertices sampled from \mathcal{C} . Then there exist $w \in (0, \frac{1}{16}]$, and a positive integer J , such that the pair $\{S_w, \mathcal{P}^J\}$ is strongly admissible for NM, where the polygonal line \mathcal{P}^J is generated by J refinement steps of the NM with the mid-point rule, starting from \mathcal{P} ,

Moreover, for any $w^* \in (0, \frac{1}{16}]$ there exists a positive integer J^* such that the pair $\{S_{w^*}, \mathcal{P}^{J^*}\}$ is strongly admissible for NM, where \mathcal{P}^{J^*} is the polygonal line generated by J^* refinement steps of the NM with S_w , starting from \mathcal{P}^J .

The advantage of using S_w with $w \neq 0$ in NMs of smooth curves is indicated by the next two results.

Result 2: Let \mathcal{C} have regularity exponent $\beta > 1$, let \mathcal{P}^0 be a polygonal line consisting of sampled points from \mathcal{C} , and let $w \in (0, \frac{1}{16}]$. If the pair $\{S_w, \mathcal{P}^0\}$, is strongly admissible for NM, then the NM with S_w as a prediction operator, starting from \mathcal{P}^0 is stable and convergent.

Moreover the details of this NM $\{d^j\}_{j \geq 0}$ decay according to

$$\|d^j\|_\infty = \max_i |d_i^j| = O(j2^{-\min(2, \beta)j}).$$

In case $w = \frac{1}{16}$ and $\beta > 3$ the details decay according to

$$\|d^j\|_\infty = O(j2^{-3j}).$$

Result 3: Let \mathcal{C} have regularity exponent $\beta > 0$. Then the NM with the mid-point prediction operator is stable and convergent.

Moreover the details of this NM decay according to

$$\|d^j\|_\infty = O(2^{-\min(2, \beta)j}).$$

It is easy to conclude from the last two results that if the smoothness of the curve is not known then the mid-point prediction operator should be used. Otherwise, the smoothness of the curve indicates which prediction operator to use, when aiming at small details and at a good approximation of the curve by the NM. Below we formulate these conclusions.

1. For a curve with regularity exponent $\beta > 3$ the details decay much faster with the predictor $S_{1/16}$ than with any other S_w with $w \in [0, \frac{1}{16})$.
2. For a curve with regularity exponent $\beta \in (2, 3]$ all prediction operators S_w with $w \in (0, \frac{1}{16}]$ are superior to the mid-point prediction, with respect to the rate of decay of the details.
3. For a curve with regularity exponent $\beta \leq 2$, the details decay much faster with the mid-point prediction operator than with any S_w with $w \in (0, \frac{1}{16}]$.

3.2.3 Normal multiresolutions with nonlinear prediction operators

Here we suggest ideas for improving the NM by using nonlinear prediction operators. We can take S^j in (58) as one of the geometry-based schemes of subsections 3.1.1 and 3.1.3.

Among these geometry-based schemes several have the advantage of being unconditionally admissible for NM, the *displacement safe 4-point* schemes due to condition (53), and the *interpolatory 4-point scheme based on circular arc approximation* by the construction of the inserted point. In fact, with the latter prediction operator the NM generates the same polygonal lines $\{\mathcal{P}^j\}$ as those generated by the NM with the mid-point prediction, but the details are different.

We conjecture that for a curve with regularity exponent $\beta > 3$, the details in the NM with the *interpolatory 4-point scheme based on circular arc approximation* as prediction operator, decay as $O(2^{-3j})$. The conjecture is based on the following observation.

Observation: Let \mathcal{C} be a curve with regularity exponent $\beta > 3$, and let the three points P_i , $i = 1, 2, 3$ be on \mathcal{C} , such that $h = \max_{i=1,2} \|P_{i+1} - P_i\|_2$ is small enough. Then the circular arc through the three points P_i , $i = 1, 2, 3$ approximates the section of the curve between these three points, with error of order $O(h^3)$. (Here the error is measured by the Hausdorff metric, which is defined in the next subsection).

3.2.4 Adaptive approximation based on the NM with mid-point prediction

Here we discuss an algorithm for the adaptive approximation of planar curves, based on the NM with the mid-point prediction operator. This algorithm is presented and analyzed in [9]. We cite here quantitative results about the quality of the approximation, expressed in terms of the number of segments in the approximating polygonal lines. The results are stated with less details and not in their full generality.

For that we introduce some notation. Let I be a segment in a polygonal line with vertices sampled from \mathcal{C} . The curve segment between the boundary vertices of I is

denoted by \mathcal{C}_I . The distance between two segments of curves γ, δ of finite length, is measured by the Hausdorff metric

$$d_{\mathcal{H}}(\gamma, \delta) = \max\{\mathcal{H}(\gamma, \delta), \mathcal{H}(\delta, \gamma)\}, \quad (62)$$

with the one-sided Hausdorff distance

$$\mathcal{H}(\gamma, \delta) = \max_{P \in \gamma} \min_{Q \in \delta} \|P - Q\|_2.$$

It is easy to see that $d_{\mathcal{H}}(\mathcal{C}_I, I) = \mathcal{H}((\mathcal{C}_I, I) \geq \mathcal{H}((I, \mathcal{C}_I)$.

Given an error tolerance ε , the adaptive algorithm refines a polygonal line \mathcal{P} with vertices sampled from \mathcal{C} , by inserting a point according to the mid-point prediction between any two vertices corresponding to a segment I of \mathcal{P} for which $\mathcal{H}((\mathcal{C}_I, I) > \varepsilon$. Once a point is inserted a detail corresponding to it is defined as in the NM with the mid-point prediction. The algorithm terminates with a polygonal line \mathcal{P} for which $\mathcal{H}(\mathcal{C}_I, I) \leq \varepsilon$ for all $I \in \mathcal{P}$. It is easy to note that the binary tree defined by this algorithm is a subtree of the binary tree generated by the NM with the mid-point prediction.

Here we cite an important result relating the number of segments in the final polygonal line obtained by the algorithm, to the error tolerance.

Result: Let \mathcal{C} be a curve with finite length, and let $\varepsilon > 0$. Denote by $\mathcal{P}(\varepsilon)$ the polygonal line generated by the algorithm with the given error tolerance, and by $|\mathcal{P}(\varepsilon)|$ the number of segments in $\mathcal{P}(\varepsilon)$. Then there exists a constant $C(\mathcal{C})$, depending on the curve, such that

$$|\mathcal{P}(\varepsilon)| \leq \frac{C(\mathcal{C})}{\varepsilon}.$$

Moreover if the curve has finite curvature, then there is a constant, $\tilde{C}(\mathcal{C})$, depending on \mathcal{C} , such that

$$|\mathcal{P}(\varepsilon)| \leq \frac{\tilde{C}(\mathcal{C})}{\varepsilon^{\frac{1}{2}}}.$$

The above result indicates that for a curve of finite length the algorithm generates polygonal lines with error decreasing linearly with the inverse of the number of segments. The error decreases as the inverse of the square of the number of segments, for curves which have a finite curvature.

References

1. Amat, S., Arandiga, F., Cohen, A., Donat, R.: Tensor product multiresolution analysis with error control for compact image representation. *Signal Processing* **82**, 587–608 (2002)
2. Amat, S., Dadourian, K., Liandrat, J.: Analysis of a class of subdivision schemes and associated non-linear multiresolution transforms. (submitted 2008), arXiv:0810.1146[math.NA]

3. Amat, S., Dadourian, K., Liandrat, J.: On a C2-nonlinear subdivision scheme avoiding Gibbs oscillations. (submitted 2008), arXiv:0812.2562[math.NA]
4. Amat, S., Donat, R., Liandrat, J., Trillo, J.C.: Analysis of a new non-linear subdivision scheme: Applications to image processing. *Found. Comput. Math.* **6**, 193–226 (2006)
5. Amat, S., Liandrat, J.: On the stability of the PPH nonlinear multiresolution. *Appl. Comput. Harmon. Anal.* **18**, 198–206 (2005)
6. Arandiga, F., Donat, R.: Nonlinear multi-scale decompositions: The approach of A. Harten. *Numerical Algorithms* **23**, 175–216 (2000)
7. Arandiga, F., Cohen, A., Donat, R., Dyn, N., Matei, B.: Approximation of piecewise smooth functions and images by edge-adapted (ENO-EA) nonlinear multiresolution techniques. *J. Comput. Harmon. Anal.* **24**, 225–250 (2008)
8. Baraniuk, R.G., Claypoole Jr., R.L., Davis, G.M., Sweldens, W.: Nonlinear wavelet transforms for image coding via lifting. *IEEE Trans. Image Process.* **12**, 1449–1459 (2003)
9. Binev, P., Dahmen, W., DeVore, R., Dyn, N.: Adaptive approximation of curves. In Dimitrov, D.K., Nikolov, G., Ulichov, R. (eds.), *Approximation Theory: a volume dedicated to Borislav Boyanov*, pp. 43–57, Martin Drinov Academic Publishing House, Sofia (2004)
10. Cavaretta, A.S., Dahmen, W., Micchelli, C.A.: Stationary subdivision. *Memoirs AMS* **93**, AMS, Providence (1991)
11. Ciesielski, Z.: Constructive function theory and spline systems. *Studia Math.* **58**, 277–302 (1975)
12. Cohen, A.: *Numerical Analysis of Wavelet Methods*. Elsevier (2003)
13. Cohen, A., Dyn, N., Matei, B.: Quasilinear subdivision schemes with application to ENO interpolation. *Appl. Comput. Harmon. Anal.* **15**, 89–116 (2003)
14. Dadourian, K.: Schemas de subdivision, analyses multiresolutions non-lineaires, applications. PhD thesis, Univerisite de Provence (2008)
15. Dahmen, W.: Wavelet and multiscale methods for operator equations. *Acta Numerica* **6**, 55–228 (1997)
16. van Damme, R.: Bivariate Hermite subdivision. *Computer Aided Geometric Design* **14**, 847–875 (1997)
17. Dyn, N., Grohs, P., Wallner, J.: Approximation order of interpolatory nonlinear subdivision schemes. *J. Comput. Appl. Math.* (2008)
18. Daubechies, I.: *Ten Lectures on Wavelets*. SIAM, Philadelphia PA (1992)
19. Daubechies, I., Runborg, O., Sweldens, W.: Normal multiresolution approximation of curves. *Constr. Approx.* **20**, 399–463 (2004)
20. Deslauriers, G., Dubuc, S.: Symmetric iterative interpolation processes. *Constr. Approx.* **5**, 49–68 (1989)
21. Donoho, D.L.: Interpolating wavelet transforms. Tech. Rep., Dep. Statistics, Stanford Univ. (2002)
22. Donoho, D.L., Yu, T.P.-Y.: Nonlinear pyramid transforms based on median interpolation. *SIAM J. Math. Anal.* **31**, 1030–1061 (2000)
23. Dyn, N.: Subdivision schemes in CAGD. In: Light, W.A. (ed.) *Advances in Numerical Analysis II*, pp. 36–104. Oxford Univ. Press, Oxford (1992)
24. Dyn, N., Floater, M.S., Hormann K.: Four-point curve subdivision based on iterated chordal and centripetal parametrization, to appear in *Computer Aided Geometric Design*, also a Technical Report no. IfI-07-06, Department of Informatics, Clausthal University of Technology (2007), Germany
25. Dyn, N., Levin, D.: Analysis of asymptotically equivalent binary subdivision schemes. *J. Comput. Appl. Math.* **193**, 594–621 (1995)
26. Dyn, N., Levin, D.: Subdivision schemes in geometric modelling. *Acta Numerica* **11**, 73–144 (2002)
27. Dyn, N., Levin, D., Liu, D.: Interpolatory convexity preserving subdivision schemes for curves and surfaces. *Computer Aided Design* **24**, 211–216 (1992)
28. Floater, M.S.: On the deviation of a parametric cubic spline interpolant from its data polygon. *Computer Aided Geometric Design* **25**, 148–156 (2008)

29. Floater, M.S., Micchelli, C.A.: Nonlinear stationary subdivision. In: Govil, N.K., Mohapatra, R.N., Nashed, Z., Sharma, A., Szabados, J. (eds.) *Approximation Theory: in memory of A. K. Varma*, pp. 209–224, Marcel Dekker (1998)
30. Goodman, T., Yu, T.P.-Y.: Interpolation of medians. *Adv. Comput. Math.* **11**, 1–10 (1999)
31. Grohs, P.: Smoothness equivalence properties of univariate subdivision schemes and their projection analogues. *Geometry Preprint 07/03*, TU Graz (2007)
32. Grohs, P.: Smoothness analysis of subdivision schemes on regular grids by proximity. *SIAM J. Numer. Anal.* **46**, 2169–2182 (2008)
33. Grohs, P.: Approximation order from stability of nonlinear subdivision schemes. *J. Approx. Th.* (submitted), also a *Geometry preprint 2008/06*, TU Graz (2008), Austria
34. Guskov, I., Vidimce, K., Sweldens, W., Schröder, P.: Normal meshes. In: Akeley, K. (ed.) *Computer Graphics (SIGGRAPH 2000: Proceedings)*, pp. 95–102, ACM Press/Addison Wesley Longman (2000)
35. Harizanov, S.: Stability of nonlinear multiresolution analysis. *Proc. Appl. Math. Mech.* **8**, 10933–10934 (2008)
36. Harizanov, S., Oswald, P.: Stability of nonlinear subdivision and multiscale transforms. *Constr. Approx.* (2009)
37. Harten A.: Discrete multiresolution analysis and generalized wavelets. *J. Appl. Numer. Anal.* **12**, 153–192 (1993)
38. Harten A.: Multiresolution representation of data: a general framework. *SIAM J. Numer. Anal.* **33**, 1205–1256 (1996)
39. Jansen, M., Baraniuk, R., Lavu, S.: Multiscale approximation of piecewise smooth two-dimensional functions using normal triangulated meshes. *Appl. Comput. Harmon. Anal.* **19**, 92–130 (2005)
40. Jia, R.-Q., Jiang, Q.: Spectral analysis of the transition operator and its application to smoothness analysis of wavelets. *SIAM J. Matrix Anal. Appl.* **24**, 1071–1109 (2003)
41. Khodakovsky A., Guskov, I.: Compression of normal meshes. In: (eds.) *Geometric Modeling for Scientific Visualization*, pp. 189–207, Springer (2003)
42. Khodakovsky A., Schröder, P., Sweldens, W.: Progressive geometry compression. In: Akeley, K. (ed.) *Computer Graphics (SIGGRAPH 2000: Proceedings)*, pp. 271–278, ACM Press/Addison Wesley Longman (2000)
43. Kuijt, F., van Damme, R.: Smooth interpolation by a convexity preserving non-linear subdivision algorithm. In: Le Mehaute, A., Rabut, C., Schumaker, L.L. (eds.) *Surface Fitting and Multiresolution Methods*, pp. 219–224, Vanderbilt Univ. Press, Nashboro TN (1997)
44. Kuijt, F., van Damme, R.: Convexity preserving interpolatory subdivision schemes. *Constr. Approx.* **14**, 609–630 (1998)
45. Kuijt, F., van Damme, R.: Stability of subdivision schemes. *TW Memorandum 1469*, Fac. Appl. Math., Univ. Twente (1998)
46. Kuijt, F., van Damme, R.: Monotonicity preserving interpolatory subdivision schemes. *J. Comput. Appl. Math.* **101**, 203–229 (1999)
47. Levin, D.: Using Laurent polynomial representation for the analysis of nonuniform subdivision schemes. *Advances of Computational Mathematics* **11**, 41–54 (1999)
48. Marinov, M., Dyn, N., Levin, D.: Geometrically controlled 4-Point interpolatory schemes. In *Advances in Multiresolution for Geometric Modelling*, Dodgson, N.A., Floater, M.S., Sabin, M.A., (eds.), pp. 301–315, Springer-Verlag (2005)
49. Matei, B.: Smoothness characterization and stability in nonlinear multiscale framework: theoretical results. *Asymptotic Analysis* **41**, 277–309 (2005)
50. Oswald, P.: *Multilevel Finite Element Approximation: Theory & Applications*. Teubner, Leipzig (1994).
51. Oswald, P.: Smoothness of a nonlinear subdivision scheme. In: Cohen, A., Merrien, J.-L., Schumaker, L.L. (eds.) *Curve and Surface Fitting (Saint Malo 2002: Proceedings)*, pp. 323–332, Nashboro Press, Brentwood TM (2003)
52. Oswald, P.: Smoothness of nonlinear median-interpolation subdivision. *Adv. Comput. Math.* **20**, 401–423 (2004)

53. Pang, J.S., Yu, T.P.-Y.: Continuous M-estimators and their interpolation by polynomials. *SIAM J. Numer. Anal.* **42**, 997–1017 (2004)
54. Ur Rahman, I., Drori, L., Stodden, V.C., Donoho, D.L., Schröder, P.: Multiscale representation of manifold-valued data. *Multiscale Model. Simul.* **4**, 1201–1232 (2005)
55. Runborg, O.: Introduction to normal multiresolution analysis. In Engquist, B., Ltstedt, P., Runborg, O. (eds.) *Multiscale Methods in Science and Engineering*, LNCSE vol. 44, pp. 205–224, Springer (2005)
56. Sabin, M.: The dual quadratic B-spline. Personal communication.
57. Sabin, M., Dodgson, N.: A circle-preserving variant of the four-point subdivision scheme. In Dahlen, M., Morken, K., Schumaker, L.L. (eds.) *Mathematical Methods for Curves and Surfaces: Tromso 2004*, pp. 275–286, Nashboro Press (2005)
58. Serna, S., Marquina, A.: Power ENO methods: a fifth-order accurate weighted Power ENO method. *J. Comput. Physics* **194**, 632–658 (2004)
59. Sweldens, W.: The lifting scheme: A custom-design construction biorthogonal wavelets. *Appl. Comput. Harmon. Anal.* **3**, 186–200 (1996)
60. Sweldens, W.: The lifting scheme: A construction of second generation wavelets. *SIAM J. Math. Anal.* **29**, 511–546 (1997)
61. Wallner, J.: Smoothness analysis of subdivision schemes by proximity. *Constr. Approx.* **24**, 289–318 (2006)
62. Wallner, J., Dyn, N.: Convergence and C^1 analysis of subdivision schemes on manifolds by proximity. *Comput. Aided Geom. Design* **22**, 593–622 (2005)
63. Xie, G., Yu, T.P.-Y.: On a linearization principle for nonlinear p -mean subdivision schemes. In: Neamtu, M., Saff, E.B. (eds.) *Advances in Constructive Approximation*, pp. 519–533, Nashboro Press (2004)
64. Xie, G., Yu, T.P.-Y.: Smoothness analysis of nonlinear subdivision schemes of homogeneous and affine invariant type. *Constr. Approx.* **22**, 219–254 (2005)
65. Xie, G., Yu, T.P.-Y.: Smoothness equivalence properties of manifold-valued data subdivision schemes based on the projection approach. *SIAM J. Numer. Anal.* **45**, 1200–1225 (2007)
66. Xie, G., Yu, T.P.-Y.: Approximation order equivalence properties of manifold-valued data subdivision schemes. (2008), to appear
67. Yang, X.: Normal based subdivision scheme for curve design. *Comput. Aided Geom. Design* **23**, 243–260 (2006)
68. Zhou, D.X.: The p -norm joint spectral radius for even integers. *Methods Appl. Anal.* **5**, 39–54 (1998)